Hybrid Internal Combustion Engine: Driving a Vehicle Using Air Compressed in Braking

by

Carlos A. Herrera

B.S., Mechanical Engineering (1996)
Massachusetts Institute of Technology

SUBMITTED TO THE DEPARTMENT OF MECHANICAL ENGINEERING
IN PARTIAL FULFILLMENT OF THE REQUIREMENTS FOR THE DEGREE OF

MASTER OF SCIENCE IN MECHANICAL ENGINEERING

AT THE

MASSACHUSETTS INSTITUTE OF TECHNOLOGY

JUNE 1998

Signature of Author.....
Department of Mechanical Engineering
May 8, 1998

Certified by.....
John B. Heywood
Sun Jae Professor of Mechanical Engineering
Thesis Supervisor

Accepted by.....
Ain A. Sonin
Chairman, Department Committee on Graduate Students

Hybrid Internal Combustion Engine: Driving a Vehicle Using Air Compressed in Braking

by

Carlos A. Herrera

Submitted to the Department of Mechanical Engineering
on May 8, 1998 in Partial Fulfillment of the
Requirements for the Degree of Master of Science in
Mechanical Engineering

ABSTRACT

After the oil crisis of the 1970's, stringent government standards placed on automobile manufacturers have led the industry to explore more fuel efficient alternatives to the vehicle with a conventional internal combustion engine/transmission powertrain. This is the motivation behind Mr. David F. Moyer's hybrid internal combustion engine concept. A vehicle using this engine should attain higher fuel economy levels as a result of kinetic energy recovery and reuse (achieved by using the engine as an air compressor during braking, storing the compressed air, and then utilizing that air to turn the engine and drive the vehicle), cylinder disabling, and the elimination of idling losses.

Data of transmission input power for Ford Motor Company's P2000 vehicle while driven through 1373 seconds of typical urban driving (CVS cycle) were used, combined with a model to estimate engine friction, to carry out an available energy analysis of the hybrid engine. An air processing efficiency was incorporated into the analysis to determine how irreversible the air storage/use processes were. Fuel economy was estimated for the different operating conditions of the concept by matching Ford's 1.8-litre Zetec engine to the vehicle and using the fuel consumption map for that engine. The vehicle with the baseline engine yields 32.6 mpg. Adding cylinder disabling raises this value to 36.8 mpg. Ultimately, if reversible hybrid operation is added, the best possible fuel economy this concept can achieve is 52.4 mpg, for a total maximum savings of 38% in fuel consumption. Using simple thermodynamic models of a braking and an air driving event, we predicted maximum values of 85% and 88% for the air processing efficiency in the braking and the air driving case, respectively. An overall value of 65% was chosen for the efficiency, resulting in a maximum fuel economy of 48.1 mpg and fuel savings of 32%.

The analysis above led us to conclude that engine friction plays a significant role in reducing the benefit of this hybrid concept. Furthermore, fully variable valve timing and cylinder disabling improve fuel economy for a conventional engine significantly, and they are essential in minimizing the thermodynamic losses involved in hybrid operation. Therefore, we recommend that methods to reduce engine friction as well as means to implement fully variable valve timing modifications to an internal combustion engine be explored further.

Thesis Supervisor: John B. Heywood
Title: Sun Jae Professor of Mechanical Engineering

Acknowledgments

Having the opportunity to work on this project and obtain useful results has been a very pleasant and filling experience. I have always had a passion for automobiles, and my participation in this project has taught me a great deal and allowed me to contribute my two cents to the car industry. My supervisor, Professor John B. Heywood, has been an invaluable resource throughout these last two years. As a teacher, both in the classroom and in project discussions, and as a researcher, Prof. Heywood has taught me many things about real problem solving and research, internal combustion engines, thermodynamics, and the automotive industry. Most importantly, though, he has taught me to always keep things in perspective and persevere, no matter how difficult the task at hand seems. My gratitude goes to him for being so committed to education, being an excellent advisor who is always willing to listen and help, and for giving me the opportunity to work with him in this project.

This project would have never happened had it not been for the impressive creativity of Mr. David F. Moyer. His hybrid internal combustion engine concept is an amazing display of ideas to improve performance, in all senses, of the automobile as we know it. I thank him very much for allowing me to benefit from his expertise and knowledge of the automobile industry. Throughout most of the duration of this project, we worked closely, and I very much appreciate his always being willing to be of assistance and the multiple times that he and his wife Pat received me at their home for discussions on the hybrid. I will always remember our conversations on all the interesting concepts he created and dealt with while working in the automobile industry.

I am extremely grateful to Mr. Bradford Bates and to his corporation, Ford Motor Company, for sponsoring this project and for allowing me to play an important role in it. His support was extraordinary, and he always made sure we got the information we needed to continue with our tasks. I will always be appreciative of the time and effort of the people at the Ford Research Laboratory who provided the data needed for our project and who were always in the disposition to answer questions give us useful feedback.

My time at the Sloan Automotive Laboratory would not have been the same without the people here. A major THANK YOU goes to my office mates, who are people I could always count on for help or advice. I thank you all for bearing with me throughout the job search process; I'm sure you are twice as happy as I am that the interviewing is all over! To my friend Robert Meyer, thanks for always listening to me and sharing your experience and wisdom. My buddies Mark Dawson and Cornelius O'Sullivan (the Irish Connection), thanks for your friendship and for all the innovative jokes. Norman Peralta... he has been gone for a year, but last year he was a wonderful source of moral support and still is a good friend. Ertan Yilmaz, I cannot thank you enough for all your useful lessons of the Turkish language; they have been very handy in defending myself... I promise Michaela Wiegel, whose name I still cannot pronounce correctly, that I'll work on my skills in German. Brad VanDerWege and Mike Shelby, I thank you guys for the help in I.C.E. related questions; you certainly know your stuff! Outside the office, everybody contributed to making the lab a better place for me. Jim Cowart has been a great friend and a very useful resource. His feedback was very valuable when the time to choose a job came around, and the discussions with him about his work in the auto industry have been very interesting. Chris O'Brien, Steven Casey, David Kayes, Derek Kim, Bertrand Lecointe, Helen Liu, Matt Rublewski, Alan Shihadeh, Dai Suzuki, and Benoist Thirouard have all been a pleasure to interact with.

I would like to thank all the staff of the lab for their help and support. Karla Stryker and Nancy Cook were always helpful and friendly. Although I did not work in the lab area, I had the opportunity to get to know and interact with Brian Corkum and Peter Menard. I thank you both for your friendship and for all the things you taught me about real car work.

Last, but certainly not least, I thank my family, particularly my mother, and all my friends for their confidence and faith in me.

Carlos A. Herrera

May 8, 1998

Table of Contents

List of Figures

List of Tables

List of Symbols

Symbol	Definition	Value/Units
bsfc	Brake specific fuel consumption	g/kW-hr
$\dot{m}_f$	Fuel flow into the engine	kg/s
$\dot{Q}$	Heat flow into control volume (CV)	W
$\dot{m}$	Mass flow rate into/out the CV	kg/s
$\dot{W}_{net}$	Net power that must be transferred to the engine	W
$\dot{W}_f$	Power dissipated inside the engine due to friction	W
$\dot{W}_T$	Power transfer from the CV to the transmission input	W
$\dot{S}_{gen}$	Rate of entropy generation inside the CV	J/s-K
W_{ava_i}	Available energy inside the tank at the beginning of a CVS second	J
W_{ava_f}	Available energy inside the tank at the end of a CVS second	J
c_p	Specific heat of air at constant pressure	1006 J/kg-K
c_v	Specific heat of air at constant volume	719 J/kg-K
E_{cv}	Energy of the air inside the tank	J
h	Specific enthalpy into/out the CV	J/kg
K	Percentage of the vehicle's energy requirement that can be delivered by the air inside the tank	
m_{cv}	Mass of air inside the tank	kg
N	Engine speed	rpm
ρ_f	Density of fuel	0.754 kg/L
P	Pressure inside the tank	Pa
P_a	Atmospheric pressure	1.0133×10^5 Pa
Q_{TOT}	Total heat transfer into the control volume	J
R	Gas constant for air	287 J/kg-K
s	Specific entropy into/out the control volume	J/kg-K
S_a	Entropy of the mass inside the tank at atmospheric conditions	J/K
S_{cv}	Entropy of the air inside the tank	J/K
s_{cv}	Specific entropy inside the tank	J/kg-K
T	Temperature of the air inside the tank	K
t	Time	s
T_a	Atmospheric temperature	300 K
tfmep	Total friction mean effective pressure	Pa
U	Internal energy of a system	J
U_a	Internal energy of the mass inside the tank at atmospheric conditions	J
V_a	Volume of the mass inside the tank at atmospheric conditions	m^3
V_T	Tank volume	m^3
W_{tank}	Actual work delivered from the tank	J
$\eta_{a,p}$	Air processing efficiency	%
$\eta_{a,c}$	Air compression efficiency	%
$\eta_{a,e}$	Air expansion efficiency	%
A_f	Frontal area of P2000 vehicle	1.98 m^2

Symbol	Definition	Value/Units
C_D	Air drag coefficient for P2000 vehicle	0.3
C_R	Coefficient of rolling resistance for P2000 vehicle	0.005
Q	General heat transfer	J
W	General work transfer	J
V	Volume of a system	m^3
S	Entropy of a system	J/K
n_{cyl}	Number of firing cylinders	
$\dot{W}$	Power transfer out of a system	W
$W_{ava_{jk}}$	Available energy of subsystem j at state k	J
u	Specific internal energy of a system	J/kg
$\dot{m}_f$	Fuel flow into the baseline engine	kg/s
$\dot{m}_{f_{HYBRID}}$	Fuel flow into the hybrid engine	kg/s
$\dot{V}_{f_{HYBRID}}$	Volumetric flow rate of fuel for hybrid engine	m^3/s
TQ_{CVS}	Second by second torque requirement of the CVS cycle	N m
τ	Time delay between torque pulses	s
TQ_{MAX}	Maximum allowable engine torque when disabling cylinders	N m
TQ_{best}	Engine torque corresponding to minimum attainable bsfc when all constraints on brake torque are considered	N m
$\dot{m}_{f\ best}$	Fuel flow into the baseline engine at TQ_{best}	kg/s
$\dot{m}^*_{f_{DSBL}}$	Fuel flow into the baseline engine under ideal cylinder disabling conditions while producing positive brake torque	kg/s
$\dot{m}^*_{f_{DSBL-HYBRID}}$	Fuel flow into the hybrid engine under ideal cylinder disabling conditions while producing positive brake torque	kg/s
$\Delta\dot{m}^*_{f_{DSBL}}$	Additional contribution to fuel flow into engine when cylinder disabling is assumed and the engine is producing positive brake torque	kg/s
$\dot{m}_{f_{DSBL}}$	Fuel flow into the baseline engine under cylinder disabling conditions while producing positive brake torque	kg/s
$\dot{m}_{f_{DSBL-HYBRID}}$	Fuel flow into the hybrid engine under cylinder disabling conditions while producing positive brake torque	kg/s
$\eta_{f,i}$	Indicated fuel conversion efficiency	%
Q_{LHV}	Lower heating value of fuel used	44.83 MJ/kg
γ	Ratio of c_p and c_v	
V_{A_k}	Cylinder volume at state k	m^3
V_B	Exhaust manifold volume	m^3
$W_{j\text{-}k}$	Net work done by the air in the cylinder in process j-k	J/cylinder-cycle
$\Lambda_{j\text{-}k}$	Relative loss of available energy in process j-k, braking event	%
$\Phi_{j\text{-}k}$	Relative loss of available energy in process j-k, air driving event	%
$\eta_{j\text{-}k}$	Efficiency of process j-k	%

Chapter 1 - Introduction

1.1 Problem Statement

A typical motor vehicle consumes energy (provided by the fuel) in several ways. In addition to the normal driving requirements of overcoming rolling resistance and aerodynamic drag, accelerating, and moving up a grade, approximately 17% of the fuel energy supplied to the engine of a mid-size vehicle is consumed due to idling of the engine at red lights, in traffic jams, and other times in urban driving. Of about 13% of the fuel energy that makes it to the drive wheels of the vehicle, 46% (equivalent to 6% of the fuel energy into the engine) is normally dissipated as heat within the brakes as they are used to slow down the vehicle [1]. Cranking the engine with an electric starter motor is an inefficient process due to the resistive losses in the electrical system of a vehicle. Throughout the years, particularly after the oil crisis of the 1970's, there has been an increasing concern to build motor vehicles that are more fuel efficient and produce less emissions, especially as the requirements imposed by the U.S. government on automobile manufacturers have become more stringent.

As a result of this, many automobile and truck manufacturers have tried a variety of concepts in their desire to attain improved fuel economy and performance. Cylinder disabling, fully variable valve timing, and various hybrid powertrains are some of these concepts, the latter being of particular interest here. For example, some bus and automobile manufacturers have attempted to implement a type of electric/fuel hybrid powertrain in which the kinetic energy of the vehicle as it decelerates is used to turn DC motors (behaving as generators under this condition) and charge a battery which is later used to transmit torque to the drive wheels via a direct drive connection between the motors and wheels. Other alternatives include the use of a flywheel to recover some of the kinetic energy of a decelerating vehicle, and the use of a fuel cell in which a combustible hydrocarbon or alcohol is reformed into hydrogen. The hydrogen-fueled duel cell is then used to power electric motors that directly drive the wheels of the vehicle, and efficiency and emissions performance could be at a level superior to that of a conventional vehicle with an internal combustion engine.

In the past, some automobile manufacturers have implemented cylinder disabling technology intending to reduce fuel consumption, but their attempts have not been completely successful. The concept of variable valve timing has been researched for many years, and its presence in automobiles has been on the rise in the last few years. In the various ways that car

makers implement this concept, it provides useful improvements in performance and fuel economy.

The purpose of this project was to provide an analytical assessment of the potential performance of a hybrid internal combustion engine concept [2] which incorporates pneumatic hybridization and cylinder disabling, along with idle shut off and no fuel consumption during braking, as its means to attain fuel economy levels superior to those of a standard automobile. Hybrid performance is achieved by using the engine as an air compressor to decelerate the vehicle, storing the compressed air in a tank, and using it to turn the engine and drive the vehicle without consuming fuel for as long as possible. Ultimately, we want to provide viable alternatives and solutions to the possible flaws encountered in its operation.

1.2 Description of Hybrid Internal Combustion Engine Concept

The hybrid internal combustion engine concept, as proposed by Mr. David F. Moyer, provides a more fuel efficient alternative to the conventional internal combustion engine/transmission vehicle powertrain. The main idea of this concept is to recover that fraction of the automobile's energy that is available at the drive wheels and is normally dissipated in the brakes (about 46% maximum in urban driving for a mid-size vehicle) by braking the vehicle by operating the engine as an air compressor and storing the compressed air in a tank. The compressed air is then used to drive the engine and the vehicle for part of its operation without consuming fuel. In addition to this primary objective, the concept includes the use of cylinder disabling, which consists of firing the minimum number of engine cylinders possible at minimum bsfc (maximum fuel conversion efficiency) to obtain the required brake torque. Idling losses are eliminated, since fuel flow is stopped whenever the vehicle is in standby mode, and unlike a conventional engine, the hybrid does not consume fuel while braking. The remainder of the time, the engine operates like a conventional 4-stroke internal combustion engine.

Figure 1-1 shows a schematic of the Moyer hybrid internal combustion engine concept. In a typical braking event, air flows into the intake manifold (IM) via valve IM_{ATM}. This air is compressed inside the cylinders whose volumes are decreasing and flows through the exhaust manifold (EM) into the storage tank via valve T_2. Throughout this process, valves T_1 and EM_{ATM} remain closed.

When powering the vehicle with compressed air, air flows from the tank into the EM (operating as the IM) via valve T_2. The pressurized air then flows into the cylinders whose volumes are increasing through their corresponding exhaust valves, performing as intake valves.

Finally, the air passes through the IM into the atmosphere after going through valve IM_{ATM}. While this occurs, valve EM_{ATM} remains shut. As we will explain in more detail later, using the exhaust side of the engine as intake during air driving is a superior choice when tailpipe emissions, efficient use of the air, and simplicity of the system are issues of concern. Ultimately, this choice allows for the connection between the tank and the IM (occurring via valve T_1) to be eliminated. When operating as an air compressor/motor, there is one braking (compression) stroke/torque pulse (expansion stroke) per engine revolution.

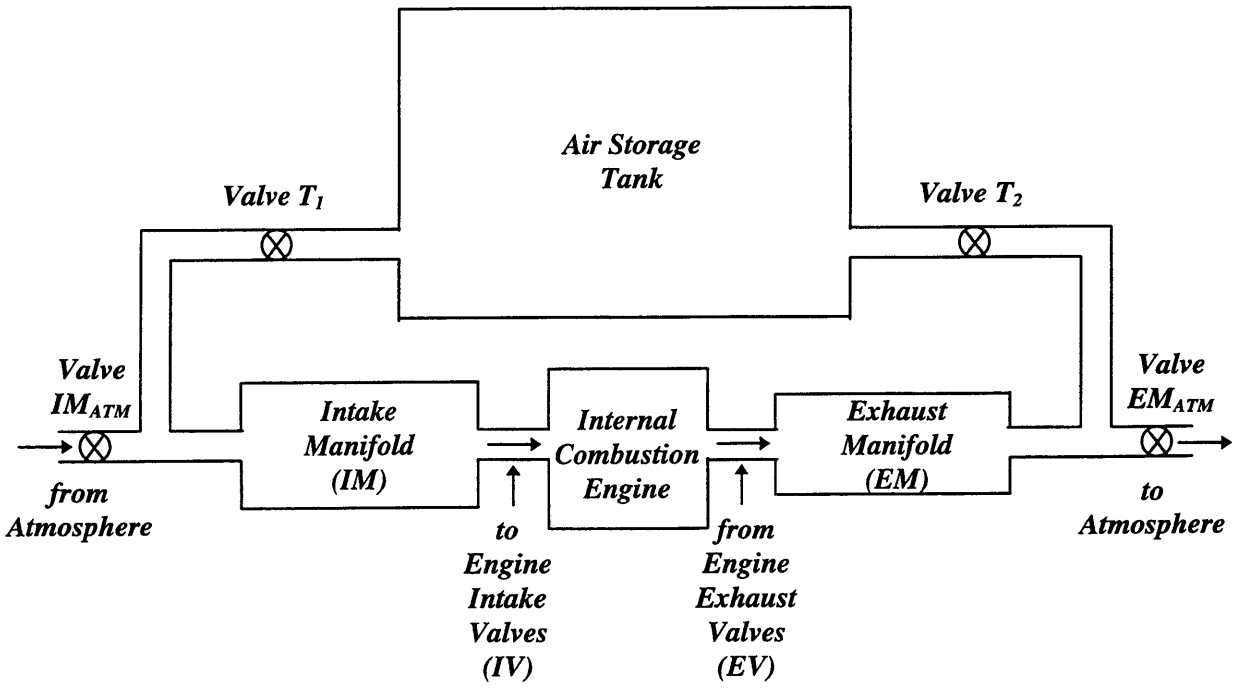

Figure 1-1. Schematic of Hybrid Internal Combustion Engine

1.3 Proposed Analysis

The hybrid internal combustion engine concept involves a wide variety of thermodynamic and fluid flow processes in its operation. When braking or powering the vehicle with air, these include gas compression and expansion processes, unrestrained expansion when pressures are equalized, and blowdown processes. Also, there are heat losses, and entropy is generated due to dissipation associated with all gas flow processes. Energy is also lost as a result of mechanical friction within the engine. Modeling each one of these processes in detail is a complex task. However, there are alternative approaches which obtain the desired information

about the performance and operation of this engine concept without the need to analyze these individual thermal-fluid processes in detail. To determine the best fuel economy attainable with this engine under different operating conditions, a fully ideal available energy analysis of the system was carried out. This was done using data obtained from Ford Motor Co. for their P2000 vehicle matched with Ford's 1.8-litre Zetec engine when driven through the CVS cycle (Federal Urban Driving Schedule).

In order to account for the thermodynamic irreversibilities resulting from the operation of the hybrid, an air processing efficiency was introduced. Air compression and air expansion efficiencies, analogous to those associated with a compressor and turbine, were used to account for energy dissipation when air is compressed and stored in the tank or extracted from the tank and expanded, respectively. After introducing these efficiencies into our ideal available energy analysis calculations, fuel economy values for the hybrid engine were estimated as a function of $\eta_{a,p}$.

Our next goal was to determine where on the air compression and air expansion efficiencies' scales the hybrid operation generally lies. Using simple models of the individual processes involved in an air braking and an air driving event, we determined where the most significant losses occurred and how some of these could be reduced. Finally, some sample calculations were run for several initial conditions to obtain estimates for the air processing efficiencies.

Engine-out and tailpipe emissions are currently a major concern to the operation of any motor vehicle. Therefore, towards the end of this work, some possible methods were examined for assessing the level of emissions attained with the hybrid internal combustion engine concept.

1.4 Ford P2000 Vehicle in the CVS Cycle

The CVS cycle is a driving schedule that represents 1373 seconds of typical city driving. It begins with a cold start. During each second, the vehicle is driven at a predetermined speed, accelerating, decelerating, and also idling. Then, following a 10 minute engine shut down and a hot start, the first 505 seconds are repeated.

For the purposes of our analysis, the data from Ford Motor Company's simulation of the P2000 vehicle over the first 1373 seconds of the CVS cycle are used. The vehicle has a mass (vehicle + payload) of 1062 kg. It has a frontal area A_f = 1.98 m^2 and air drag and rolling resistance coefficients of C_D = 0.3 and C_R = 0.005, respectively.

Based upon this information and other characteristics of the vehicle, estimates were made of the power and torque required at the transmission input to accelerate or brake the vehicle in accordance to the requirements of the CVS cycle at every second. Knowledge of the transmission's gear ratios also allowed the engine speed to be computed at each second. These numbers were generated at Ford Motor Co. assuming that there was neither an engine nor customary friction brakes in the vehicle. Consequently, all braking and accelerating of the P2000 vehicle in this simulation were done through the input shaft of the transmission.

Chapter 2 - Available Energy Analysis

2.1 Concept of Available Energy

Available energy is the maximum amount of work that can be extracted from a system (air in this case) at a given state when it attains equilibrium with an atmosphere. Starting from a given set of initial properties of stored air, where three of the properties pressure, temperature, volume, and mass are defined, a reversible (ideal) expansion is assumed in which the air ends at atmospheric pressure and temperature. The net amount of work extracted during this ideal expansion represents the maximum work that can be obtained from the initial system/atmosphere configuration through the utilization of fully reversible machinery.

For a closed system with mass m, initial temperature T, initial internal energy U, and initial entropy S, which is stored in a volume V_T, absorbing an amount of heat Q from the atmosphere at temperature T_a, and delivering an amount of work W, the first and second laws of thermodynamics, and the ideal gas law yield,

$$\begin{aligned} Q - W &= U_a - U = mc_v\left(T_a - T\right) \\ S_a - S &= \frac{Q}{T_a} + S_{gen} \\ PV_T &= mRT \\ P_a V_a &= mRT_a \end{aligned} \qquad (2.1)$$

The maximum amount of work is obtained when $S_{gen} = 0$. After substituting this into Eqs. (2.1), we get

$$W = T_a\left(S_a - S\right) - \left(U_a - U\right). \qquad (2.2)$$

However, the air inside the tank does some work in displacing the atmospheric air around it. Consequently, the maximum useful work, that is, the available energy of the stored air, is given by

$$W_{ava} = \left(U - U_a\right) + P_a\left(V_T - V_a\right) - T_a\left(S - S_a\right). \qquad (2.3)$$

This result represents the best that can be done with the given stored air.

Irreversible work transfers into a system increase the system's available energy by an amount less than their magnitude, while those out of a system decrease that quantity by an amount larger than their magnitude. The differential change in available energy dW_{ava} resulting from a net heat transfer δQ into the system is given by

$$dW_{ava} = \left(1 - \frac{T_a}{T}\right)\delta Q, \tag{2.4}$$

since in addition to heat, entropy is transferred through the boundary [3]. Reversible work transfers change available energy by their exact value. This is the case of interest in this chapter.

2.2 Engine Friction

As we described in Chapter 1, the CVS cycle simulation results of torque required at the transmission input utilized in our analysis do not account for the presence of an engine. Consequently, the figures representing power at the transmission input at each second of the cycle do not include the effect of engine friction. To obtain a more accurate estimate of how much compressed air can be produced or used throughout the CVS cycle, the friction within the engine must be accounted for, since the engine is the compressor and expander.

For typical small automotive 4-stroke, 4-cylinder spark-ignited engines, the total friction mean effective pressure (tfmep) at wide open throttle under motoring conditions, which represents friction wok dissipated per cycle per unit of engine displacement volume, is given by

$$tfmep = \left[0.97 + 0.15\left(\frac{N}{1000}\right) + 0.05\left(\frac{N}{1000}\right)^2\right] \times 10^5, \tag{2.5}$$

where N is the engine speed in revolutions per minute, and *tfmep* is given in Pa [3]. This historical model, however, overestimates the engine friction in modern engines. A more recent model and set of data [4] indicate that current engines have about 75% of the friction that Eq.(2.5) predicts. Therefore, for our thermodynamic analysis of the system, *tfmep* given by Eq.(2.5) was scaled by 0.75.

To calculate the friction dissipation inside the engine, *tfmep* must be multiplied by the engine's displacement, 1796 cm^3 for the Zetec engine, to obtain friction work per cycle. This number, in turn, must be divided by 2 to get friction work per revolution, and finally multiplied by engine speed to obtain units of power. The final expression for friction power in Watts is

$$\dot{W}_f = 4(tfmep)V_d \frac{N}{2}, \tag{2.6}$$

where V_d is the displaced volume of one engine cylinder.

Engine friction has a significant effect on the amount of air that can be stored inside the tank. For light vehicle braking rates, during which the vehicle's velocity decreases slowly, the amount of power dissipated due to engine friction is greater in magnitude than that which must be absorbed from the transmission input. In order for the automobile not to slow down at a rate

larger than required by the FUDS (Federal Urban Driving Schedule), power must be delivered to the engine's pistons instead of absorbed from them. In the case of a standard engine, this power demand is met by firing the engine, but in the case of the hybrid, it is met preferably by the controlled release of compressed air into the engine's cylinders, since this results in fuel savings.

2.3 Description of Available Energy Analysis

Figure 2-1 shows a physical model of the hybrid internal combustion engine concept. It includes an internal combustion engine with an intake manifold, an exhaust manifold and an air tank with volume V_T. All these are enclosed within a control volume, denoted by the dashed line. The device is surrounded by the atmosphere. As air flows from the tank through the engine and manifolds, and out to the atmosphere, mechanical power of magnitude $\dot{W}_T$ is transmitted to the drive shaft by the engine. During this process, a heat flow of magnitude $\dot{Q}$ is absorbed from the atmosphere. The reverse process occurs when power is transferred to the engine's drive shaft. Then air from the atmosphere is pumped into the tank by the engine. During this process, energy is lost as heat to the surroundings.

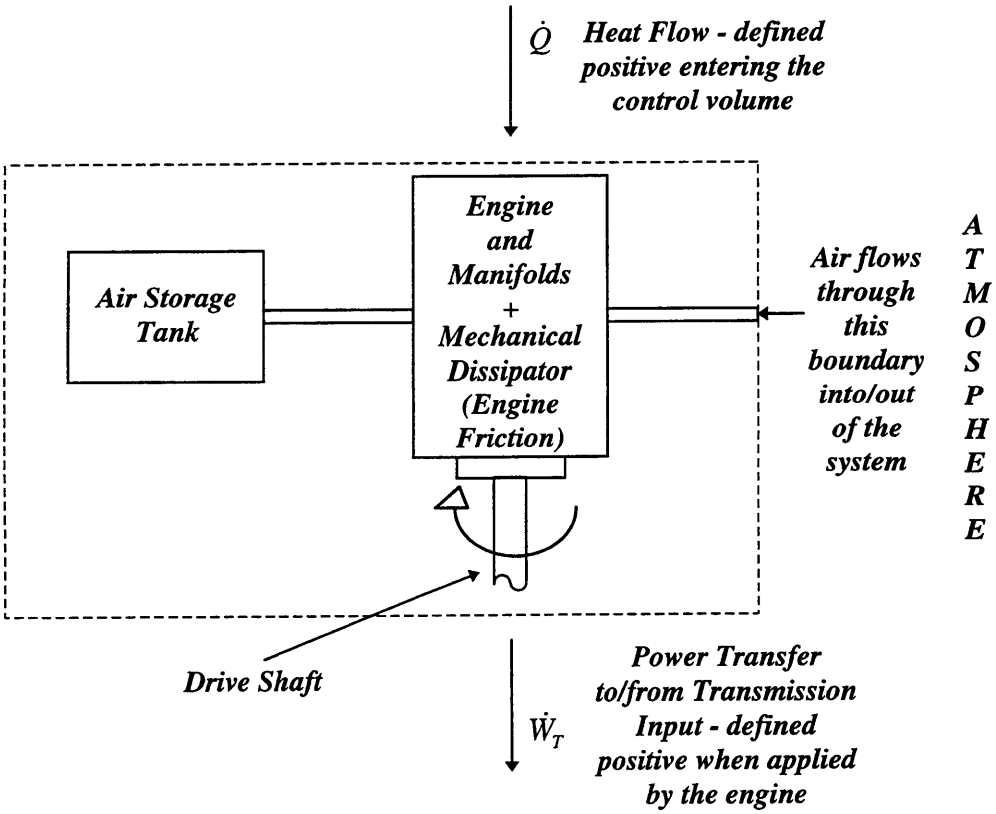

Figure 2-1. Hybrid Internal Combustion Engine Physical Model

In order to determine the best fuel economy level attainable with the hybrid system in the configuration shown above, idealized versions of the real processes were used for our analysis. Therefore, it was assumed that the power at the transmission input (negative when it is available for absorption and positive when it must be transmitted) added with the power dissipated due to friction (positive, since it always represents a loss) was delivered or extracted in full as available energy to or from the tank. Then, the amount of power that must be delivered to the engine input (from the tank or by providing fuel) or delivered to and stored in the tank is given by

$$\dot{W}_{net} = \dot{W}_T + \dot{W}_f \,. \tag{2.7}$$

The detailed flow, blowdown, and other time dependent processes involved were not included in the analysis.

The available energy analysis described above is fully ideal. However, the true processes involved in storing and using air are not reversible. As air is pumped into the tank or withdrawn from it, available energy is lost as a result of a combination of blowdown and mixing processes and heat losses. Therefore, the ideal results presented at the end of this chapter and in Chapter 4 must be modified to account for the additional sources of dissipation.

The losses involved in the storage and utilization of air are accounted for by introducing an air processing efficiency, $\eta_{a,p}$, into the ideal available energy analysis model. An air compression efficiency, $\eta_{a,c}$, and an air expansion efficiency, $\eta_{a,e}$, which are analogous to compressor and turbine efficiencies, are used for the air storage and air use cases, respectively.

In the case that air is stored into the tank, the amount of power that is stored in the form of available energy is now defined as

$$\dot{W}_{net} = \eta_{a,c}\left(\dot{W}_T + \dot{W}_f\right), \text{ for } \dot{W}_{net}, \dot{W}_T < 0\,. \tag{2.8}$$

Similarly, when air has to be extracted from the tank, either because the vehicle must accelerate or because it must decelerate at a very small rate (power dissipation in the engine exceeds power available at the transmission input), we have that

$$\begin{aligned} \dot{W}_T &= \eta_{a,e}\dot{W}_{net} - \dot{W}_f \;\Leftrightarrow \\ \dot{W}_{net} &= \frac{1}{\eta_{a,e}}\left(\dot{W}_T + \dot{W}_f\right), \text{ for } \dot{W}_{net} > 0 \end{aligned} \tag{2.9}$$

There are two bounding cases of reversible (no loss) thermodynamic processes. In an adiabatic process, everything takes place at a fast enough rate for heat transfer to be considered negligible. In an isothermal process, enough time is assumed to be available for sufficient heat

transfer to occur to maintain the temperature of the system constant throughout the whole process. The results of any practical process lie between these two cases. However, since what is being carried out is an available energy analysis, our choice of processes will not affect the final estimates of steady-state fuel economy. The difference between the reversible adiabatic case and the reversible isothermal case is that at each second of the CVS cycle, the pressure and temperature of the air in the tank will be different for each type of process.

For the control volume (dashed line) in Fig. 2-1, the first law of thermodynamics is

$$\frac{dE_{cv}}{dt} = \dot{Q} - \dot{W} + \sum (\dot{m}h)_{in} - \sum (\dot{m}h)_{out} . \tag{2.10}$$

The second law states that

$$\frac{dS_{cv}}{dt} = \sum \frac{\dot{Q}}{T_a} + \sum (\dot{m}s)_{in} - \sum (\dot{m}s)_{out} + \dot{S}_{gen} , \tag{2.11}$$

where $\dot{S}_{gen} = 0$ for a reversible process. Lastly, the ideal gas law gives

$$PV_T = m_{cv} RT . \tag{2.12}$$

These equations are developed further in Appendices A and B into the forms that they are used in to compute the state of the air at the end of each second of the CVS cycle.

2.3.1 Reversible Adiabatic Processes

The assumption of reversible adiabatic processes implies that when the hybrid engine operates, air will be pumped into the tank or removed from it without any heat losses or entropy generation. In order for this presumption to be valid, the time constants of the processes in question must be small. That is not the situation with the current setup. The time constants of most of the internal fluid flow processes occurring in the hybrid engine are on the order of 20-30 ms, whereas the frequency at which events take place inside the tank is on the order of 1 second. Heat losses in the cylinder, intake, and exhaust systems are known to be a problem in the operation of an internal combustion engine, another issue that questions the validity of the assumption of adiabatic processes.

2.3.2 Reversible Isothermal Processes

As discussed above, idealizing the storage and use of available energy as a set of reversible isothermal processes is appropriate when the time scale in which events take place in the tank is large enough, allowing for sufficient heat transfer to maintain the temperature of the air at atmospheric conditions throughout the whole process. As before, no entropy is generated.

In addition to their being more realistic than the adiabatic no heat transfer assumption, reversible isothermal processes were used as the basis of our available energy analysis due to their additional simplicity, as a comparison of Appendices A and B shows.

The storage and removal of air is governed by the equations

$$\begin{aligned} V_T\left(P_i \ln\frac{P_i}{P_a} - P_f \ln\frac{P_f}{P_a}\right) - W_{tank} &= \left(P_i - P_f\right)V_T \\ T_f &= T_i \\ m_{cv_f} &= m_{cv_i}\frac{P_f}{P_i} \end{aligned} \quad , \tag{2.13}$$

where the variables with the subscripts i and f represent the values of the corresponding parameters at the beginning and end of a second in the CVS cycle, respectively. The temperature is assumed to be such that $T = T_i = T_f = T_a$. The heat transfer into the system is given by

$$Q_{TOT} = V_T\left(P_i \ln\frac{P_i}{P_a} - P_f \ln\frac{P_f}{P_a}\right). \tag{2.14}$$

The derivation of Equations (2.13) and (2.14) is described in more detail in Appendix B.

2.4 Energy Demand of Vehicle in the CVS Cycle

The FUDS contains 764 sec of driving/accelerating, 262 sec of idling of the engine, and 347 sec of braking/decelerating. Throughout the 1026 sec of idling and accelerating combined, energy must be provided to the engine to overcome engine friction, and as needed, to overcome aerodynamic drag, rolling resistance, and accelerate the vehicle. However, it turns out that for 138 sec out of the 347 sec of braking, energy must also be provided to the engine (in the form of fuel or compressed air) because friction dissipation within the engine exceeds the magnitude of the power at the transmission input. Under typical operating conditions, available energy may be stored in the tank for 209 sec, approximately 15% of the time that the P2000 vehicle with the 1.8-litre Zetec engine is driven in the CVS cycle. If there were no engine friction, the 15% figure would become 25%, illustrating the significance of engine friction.

Assuming reversible isothermal processes, the pressure inside the tank was calculated at each second of the CVS cycle as energy was transferred to/from the tank for several operating configurations. Figure 2-2 and 2-3 show the history of the air pressure in the tank for seconds 100 through 700 of the CVS cycle when idle shut off is used for air processing efficiencies of 100% and 65%, respectively. The latter was chosen as an example because it is a typical value

for mechanical compressors and turbines. In the fully ideal case, a peak tank pressure of 10 atm is reached in the 331st second, while in the 65% case, the peak pressure is approximately 7.5 atm. The graphs also show how frequently the tank is charged/discharged due to the variability in the power requirements of the cycle.

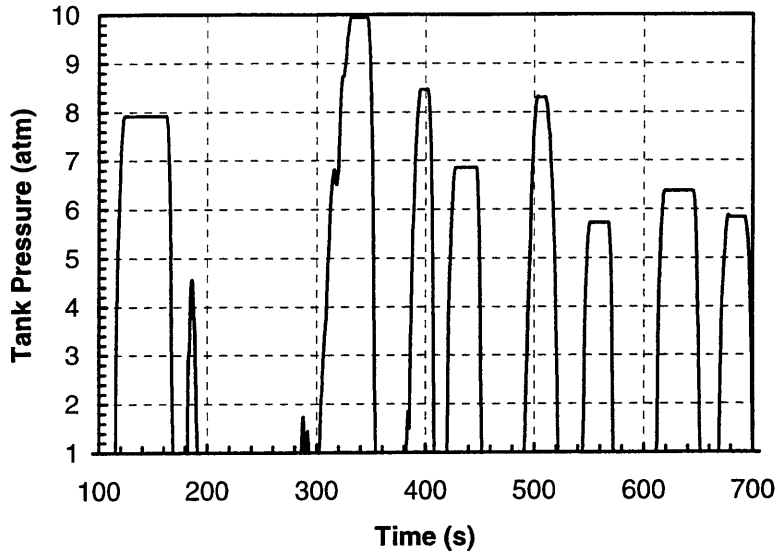

Figure 2-2. Tank Pressure vs. Time in the CVS Cycle with Engine Idle Shut Off, $\eta_{a,p}$=100%

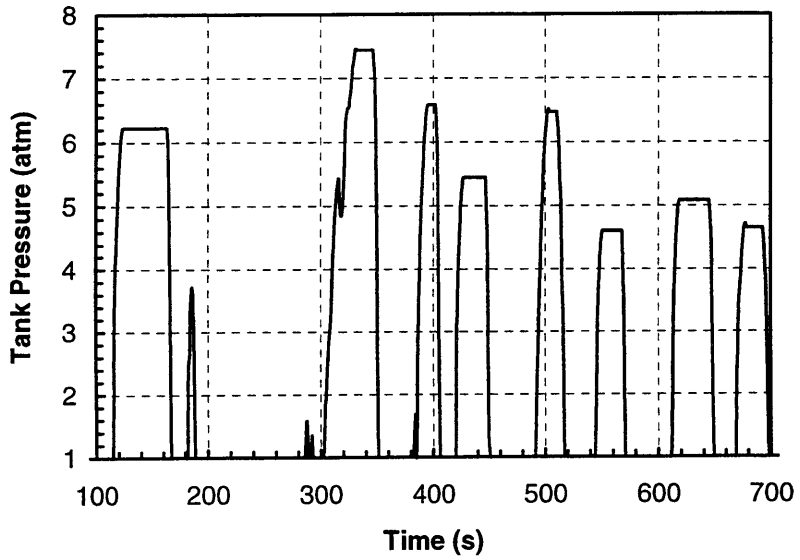

Figure 2-3. Tank Pressure vs. Time in the CVS Cycle with Engine Idle Shut Off, $\eta_{a,p}$ = 65%

At each second, the available energy of the air inside the tank was monitored. This was done to ensure that the changes in this quantity matched exactly the amount of energy transmitted

to the engine or absorbed from it as determined by Eqs.(2.8) and (2.9). Most importantly, though, this amount was checked to determine if the contents of the tank had enough energy to power the vehicle through a given second.

As a result of this, we obtain that the actual work transfer out of the tank, W_{tank}, during that second is

$$W_{tank} = \begin{Bmatrix} \dot{W}_{net} \times 1\text{sec}, \ if \ \dot{W}_{net} < 0 \\ \dot{W}_{net} \times 1\text{sec}, \ if \ 0 < \dot{W}_{net} \times 1\text{sec} < W_{ava_t} \\ W_{ava_t}, \ if \ \dot{W}_{net} \times 1\text{sec} > W_{ava_t} \end{Bmatrix}, \tag{2.15}$$

where W_{ava_t} is the available energy inside the tank at the beginning of the second of interest in the cycle. In the case that the available energy inside the tank is not enough to power the vehicle through a given second, the fraction of the energy requirement that the air inside the tank can provide is computed. It is

$$K = \frac{W_{ava_t}}{\dot{W}_{net} \times 1\text{sec}}. \tag{2.16}$$

2.5 Estimating Fuel Consumption

The main objective of the hybrid internal combustion engine concept is to achieve significantly higher fuel economy values than those attainable by utilizing a conventional engine. The fuel savings arise from the recovery of some of the vehicle's kinetic energy during braking, from the elimination of idling losses, and from cylinder disabling, which is described in more detail in Chapter 3. The goal is to store as much energy as possible during braking in the form of compressed air and to later use that air to drive the vehicle in lieu of fuel.

Using data of fuel flow versus engine speed and brake torque for Ford's 1.8-litre Zetec engine and the results from our ideal available energy analysis of the P2000 vehicle in the CVS cycle, fuel consumption was determined at each second for the baseline vehicle and the vehicle with the hybrid engine under various configurations: allowing the engine to idle when it is supposed to (using compressed air when possible), shutting the engine off when the CVS cycle calls for idling, and neglecting engine friction. The total amounts of fuel consumed were then compared to determine the total fuel savings. Finally, steady-state fuel economy (in miles per gallon, mpg) was calculated for each scenario. All these figures were obtained using an 80 liter air storage tank. This is the size suggested by the inventor of the concept, and the choice does

not affect the vehicle's fuel consumption, since we are carrying out an available energy analysis. It affects, however, the time history of the tank pressure.

2.5.1 Braking the Vehicle

When the brakes are applied on a typical motor vehicle, the engine continues to fire and thus consume fuel. With the hybrid engine, however, this would not be the case. Fuel flow would stop whenever there is no need for the engine to produce positive brake torque. Consequently, the use of this system results in fuel savings obtained while braking the vehicle.

By definition, engine torque is negative when it is absorbed. The fuel consumption map obtained from Ford Motor Co. contains no data on fuel flow into the engine for zero or negative values of torque. The numbers begin at small (close to zero) values of brake torque and continue to much larger values. Therefore, it was assumed that when the engine was utilized to slow the automobile down, the engine torque was approximately zero. Fuel flow values at each engine speed corresponding to points of very small torque were chosen, and a quadratic curve fit of fuel flow versus engine speed was done.

The relation between fuel flow and engine speed at approximately zero torque was estimated to be

$$\dot{m}_f \approx 2.387 \cdot 10^{-11} N^2 + 1.163 \cdot 10^{-7} N + 2.981 \cdot 10^{-5}, \tag{2.17}$$

where fuel flow $\dot{m}_f$ is given in kg/s, and N is in rpm. Figure 2-4 shows a comparison between the actual data and those predicted by the polynomial curve fit.

The mass of fuel that could potentially be saved (that consumed by the conventional engine) in a second of the CVS cycle in which engine torque is negative is obtained by multiplying the result from Eq.(2.17) by 1 sec. For a braking event in which the magnitude of the power from the transmission is smaller than the amount of dissipation within the engine, the mass and volume of fuel consumed by the hybrid per second are calculated, respectively, via

$$\begin{aligned} \dot{m}_{f_{HYBRID}} &= (1-K) \times \dot{m}_f \\ \dot{V}_{f_{HYBRID}} &= \frac{\dot{m}_{f_{HYBRID}}}{3.785 \times \rho_f} \end{aligned}, \tag{2.18}$$

where ρ_f is the fuel's density. The value of K is obtained from Eq.(2.16). When the magnitude of the power delivered from the transmission exceeds the amount dissipated within the engine, $K = 1$, and as expected, the hybrid consumes no fuel.

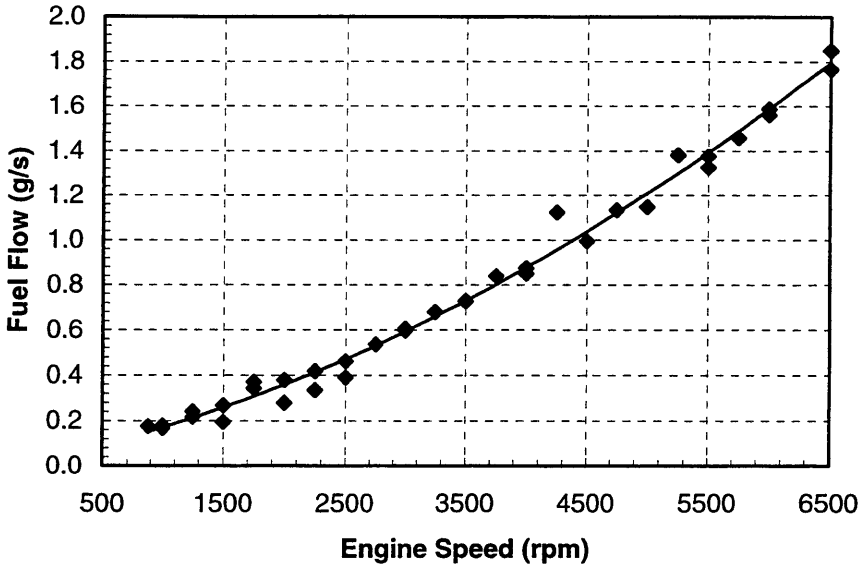

Figure 2-4. Fuel Flow vs. Engine Speed at Approximately Zero Engine Brake Torque

2.5.2 Accelerating the Vehicle

Whenever the velocity of the P2000 vehicle must be increased, the engine must transmit torque and power to the transmission. In a standard automobile, fuel must be provided to the engine in order to obtain brake torque from it. With the hybrid internal combustion engine, we fulfill as much of the vehicle's power requirement as possible using compressed air as a source of energy.

The fuel consumption map for Ford's 1.8-litre Zetec engine contains data on fuel flow as a function of both engine speed and brake torque. As discussed above, the values for these two parameters are known at each second of the CVS cycle simulation. Consequently, the fuel flow figures were interpolated (linearly) within appropriate brake torque values and finally between the known engine speed values that bounded the actual numbers from the CVS cycle. This procedure resulted in the desired parameter, fuel flow, $\dot{m}_f$, at a specific engine torque and speed point. The amount of fuel consumed by the hybrid engine is again given by equations (2.16) and (2.18).

2.6 CVS Cycle Results

Ford Motor Co.'s P2000 vehicle is driven for 11.9 km (7.45 miles) for the 1373 seconds of the CVS cycle. Results of steady-state fuel consumption/economy were generated for the

baseline vehicle with the 1.8-litre Zetec engine, and for the hybrid version of it under three sets of conditions: choosing to idle the engine with air when it is scheduled to idle, shutting the engine off at idle, and neglecting engine friction. The latter was done to determine the impact of reduced engine friction. This was done for several values of the air processing efficiency ranging from 100% (fully reversible case) to 0% (no air storage/use capability).

Any difference in stored energy between beginning and end of the CVS cycle affects fuel consumption, and thus, the savings realized. So, a boundary condition was imposed such that the pressure inside the storage tank is the same at the end of the 1372nd second than it is at the 0th second of the CVS cycle. The tank behaves like a "battery" that has undergone no net change in its energy level by the end of the cycle. Likewise, the vehicle begins and ends the FUDS with zero velocity. Table 2-1 shows the steady-state tank pressure, mass of fuel consumed, relative reduction in fuel consumption, and fuel economy for different setups of the hybrid internal combustion engine operating reversibly.

Table 2-1. Results of Ideal Available Energy Analysis vs. Mode of Operation of Hybrid Internal Combustion Engine

Mode of Operation	Steady-State Pressure (atm)	Mass of Fuel Used (g)	Reduction Relative to Baseline (%)	Fuel Economy (mpg)
Baseline, 1.8-litre Zetec Engine		***651.3***		***32.6***
Hybrid, Idle the Engine	*3.33*	*490.6*	*25*	*43.3*
Hybrid, Do not Idle	*3.97*	*469.5*	*28*	*45.3*
Hybrid, No Engine Friction	*5.65*	*333.8*	*49*	*63.7*

Introducing hybrid operation into the baseline P2000 vehicle with Ford's 1.8-litre Zetec engine results in 25% less fuel consumption, an increase in fuel economy from 32.6 mpg to 43.3 mpg. If idle shut off is an option (in addition to hybridization), fuel usage drops by an additional 3%, and the vehicle yields an additional 2 mpg. If engine friction could be reduced to zero, the mass of fuel consumed would be an additional 21% less than the best fuel consumption attainable with the hybrid, a total reduction of 49% relative to the baseline automobile. Fuel economy would reach a high value of 63.7 mpg. The significance of engine friction in reducing the benefit of this concept becomes evident after examining the results above. If friction were reduced by 30%, the 43.3 mpg figure corresponding to the hybrid with idle would climb to 45.9 mpg, while the economy corresponding to the hybrid without idle would increase to 47.4 mpg, a reduction in fuel consumption of 31% relative to the baseline.

We want to determine how changes in the air processing efficiencies affect the improvement in hybrid steady-state fuel economy. The graph in Fig. 2-5 shows steady-state fuel economy relative to that of the P2000 vehicle with the baseline 1.8-litre Zetec engine. The results were generated using the definitions of work in Eqs.(2.7) through (2.9).

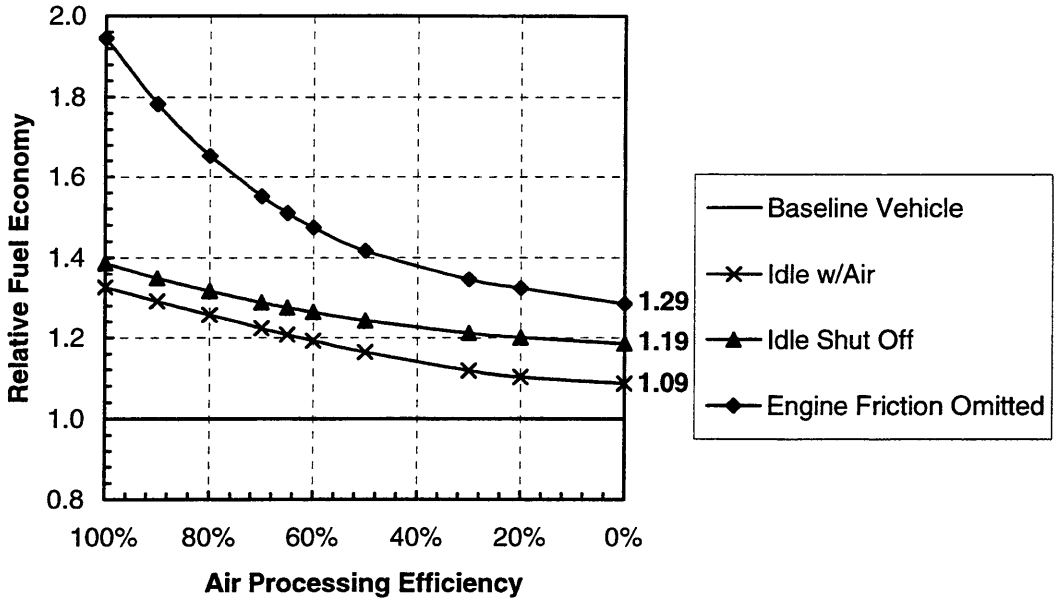

Figure 2-5. Relative Steady-State Fuel Economy vs. Air Processing Efficiency - Simple Hybrid

One point that stands out of these graphs is that at 0% efficiency, where the pneumatic hybrid is not accomplishing anything, there is still a relative fuel economy benefit. Introducing fully irreversible hybrid operation into the baseline vehicle results in a 9% improvement in steady-state fuel economy. This is caused by the fact that, when the hybrid system is in place, no fuel is injected into the engine during braking. If idle shut off is then added to the hybrid, the relative benefit becomes 19%. Ultimately, if engine friction were negligible, the elimination of braking and idling fuel results in a 29% improvement. The reduction in fuel consumption for the three cases is 8%, 16%, and 22%, respectively. Of these, only the benefit of no fuel injection during braking is inherent in the hybrid. Fuel shut off at idle can be done with the standard engine. Reduced engine friction would obviously benefit the standard engine as well.

Chapter 3 - Cylinder Disabling

3.1 Overview

Besides hybrid operation, no fuel usage during braking, and engine shut off at idle, the concept of cylinder disabling also contributes significantly to improved fuel economy. The main idea behind disabling is to fire less than all 4 cylinders in the 1.8-litre Zetec engine whenever possible. In this manner, instead of firing the whole engine at a given, relatively high bsfc, fewer cylinders would be fired at conditions as close to minimum bsfc (maximum fuel conversion efficiency) as achievable. The details of this idea as well as some of the constraints and limitations associated with its implementation are discussed in further detail in the subsequent sections. Furthermore, the effect that engine friction has on fuel consumption when disabling cylinders is also explored.

3.2 Limitations on Minimum bsfc Operation

When implementing cylinder disabling, the firing engine cylinders would ideally be operating at minimum bsfc. However, there are several factors that cause performance to deviate from the ideal. The brake torque provided by the engine with disabled cylinders at maximum efficiency must be at least as large as the torque requirement at each second of the CVS cycle. If this is not the case, the engine will have to operate at a higher bsfc level which meets the torque demand of the FUDS, TQ_{CVS}.

In order to ensure smooth driving conditions, the time between each engine torque pulse, τ, must remain relatively small. This requirement may also result in the engine firing at less than maximum efficiency conditions during several seconds of the CVS cycle. For a 4-cylinder engine, the number of cylinders that must fire (per cycle) during a given second of the FUDS is given by

$$n_{cyl} = 4\frac{TQ_{CVS}}{TQ_{best}}, \tag{3.1}$$

where TQ_{best} is the engine torque corresponding to as close to minimum bsfc as possible at a given engine speed. The number of torque pulses per unit time is then governed by

$$\frac{1}{\tau} = n_{cyl} \cdot \frac{1\text{ cycle}}{2\text{ rev}} \cdot \frac{N\text{ rev}}{\text{min}} \cdot \frac{1\text{ min}}{60\text{ sec}} = \frac{N}{30} \cdot \frac{TQ_{CVS}}{TQ_{best}}. \tag{3.2}$$

Therefore, the time delay between torque pulses, in seconds, is

$$\tau = \frac{30}{N} \cdot \frac{TQ_{best}}{TQ_{CVS}}. \tag{3.3}$$

In order to fulfill the driveability constraint, we must have

$$TQ_{best} \leq TQ_{MAX} = \frac{N}{30} \cdot TQ_{CVS} \cdot \tau. \tag{3.4}$$

For the purpose of our analysis, τ was chosen to be 0.11 seconds. This constraint was applied in all our calculations of fuel consumption using cylinder disabling. It results in an increase in fuel consumption in the CVS cycle of 8.55 g of fuel (2.9%) for the baseline 1.8-litre Zetec engine relative to the case with no driveability constraint.

Equation (3.2) reveals that, in general, n_{cyl} is not an integer. The question that follows is: how can a non-integral number of cylinders be disabled? According to David Mover's theory of operation of the hybrid internal combustion engine concept, this is feasible. In a second of the CVS cycle, a different number of cylinders would fire during each engine cycle in a way such that at the end of the second, the engine has produced the required mean amount of brake torque. For example, if at a given second Eq.(3.2) indicates that 2.5 cylinders must fire, 3 cylinders would fire for a few cycles and 2 cylinders would do so for several other cycles in a way that the torque requirement of the FUDS is met. It is not clear, though, whether this would be smooth enough to be transparent to the driver of the vehicle.

3.3 Estimating Fuel Consumption

3.3.1 Real Case Description and Steady-State Results

As discussed in Section 2.5.2, the fuel consumption map for the 1.8-litre Zetec engine relates values of fuel flow and bsfc to engine speed and brake torque. In order to determine the maximum fuel economy attainable when using cylinder disabling in driving, the brake torque and fuel flow rate values were sorted in order of increasing bsfc for each engine speed in the map. At each second of the FUDS in which energy must be provided to the engine, the engine speed is known. Consequently, the next step was to choose engine speed values that bounded the actual value, and to pick (at each one of these two speeds) the minimum bsfc (or closest to minimum bsfc points) as dictated by the conditions on torque described in Section 3.2. Ultimately, the fuel flow and brake torque values at the two chosen points were interpolated linearly within the bounding values of engine speed. From this procedure, we determined the fuel flow, $\dot{m}_{f_{best}}$, and

the brake torque, TQ_{best} (positive), corresponding to maximum efficiency (or as close to it as possible) as a function of engine speed in the CVS cycle.

When the 1.8-litre Zetec engine is firing, generating a net positive brake torque, and some cylinders are disabled, the pistons in the non-firing cylinders continue to translate. Although there is no combustion taking place inside the disabled cylinders, it takes energy to move the corresponding pistons and overcome the friction losses associated with them. The fulfillment of this energy requirement results in additional fuel consumption, which increases bsfc.

The fuel consumed by the baseline 1.8-litre engine when producing positive brake torque, engaging in cylinder disabling, and neglecting the effect of friction in the disabled cylinders is given by

$$\dot{m}^{*}_{f_{DSBL}} = \frac{n_{cyl}}{4} \cdot \dot{m}_{f_{best}} . \tag{3.5}$$

The additional mass of fuel consumed due to friction in the disabled cylinders is estimated via

$$\Delta\dot{m}^{*}_{f_{DSBL}} = \frac{\dot{W}_f \cdot 1\ \text{sec}}{1000 \cdot Q_{LHV} \cdot \eta_{f,i}} \cdot \left(1 - \frac{n_{cyl}}{4}\right), \tag{3.6}$$

where the indicated fuel conversion efficiency, $\eta_{f,i}$, was set equal to a typical value of 35%. Consequently, the total fuel flow for the conventional engine while engaging in cylinder disabling and producing positive brake torque is

$$\dot{m}_{f_{DSBL}} = \dot{m}^{*}_{f_{DSBL}} + \Delta\dot{m}^{*}_{f_{DSBL}} . \tag{3.7}$$

The mass and volume consumed by the hybrid when cylinder disabling is used are calculated, respectively, through

$$\begin{aligned} \dot{m}_{f_{DSBL-HYBRID}} &= (1-K) \times \dot{m}_{f_{DSBL}} \\ \dot{V}_{f_{DSBL-HYBRID}} &= \frac{\dot{m}_{f_{DSBL-HYBRID}}}{3.785 \times \rho_f} \end{aligned} . \tag{3.8}$$

If the engine is absorbing torque from the transmission, and the magnitude of the power delivered from the transmission exceeds the amount dissipated within the engine, fuel flow is governed by Eq.(2.17). In the event that there is more dissipation than there is power to absorb from the transaxle, fuel flow is then determined by using Equations (2.16) through (2.18).

Table 3-1 shows the mass of fuel consumed, the reduction in fuel consumption relative to the no cylinder disabling case, and fuel economy for different setups of the hybrid internal combustion engine when used in conjunction with cylinder disabling and operating at

$\eta_{a,p}$ = 100%. The results account for full friction in the non firing cylinders. The utilization of cylinder disabling on the P2000 vehicle with the hybrid internal combustion engine concept (using the 1.8-litre Zetec engine as baseline) results in significant improvements in fuel economy. The baseline engine with cylinder disabling consumes 11% less fuel than the standard engine, which represents an increase in predicted fuel economy from 32.6 mpg to 36.8 mpg. The best performance attainable with this engine concept is 52.4 mpg, which corresponds to using hybrid operation combined with disabling and with turning the engine off at idle. This represents 38% less fuel usage than that for the Zetec engine with no modifications. If engine friction were reduced by 30%, the concept would yield a maximum fuel economy of 60.4 mpg in its hybrid with cylinder disabling and idle shut off configuration, for an improvement in fuel consumption of 13% relative to its full friction counterpart.

Table 3-1. Results of Ideal Available Energy Analysis vs. Mode of Operation of Hybrid Internal Combustion Engine with Cylinder Disabling

Mode of Operation	Mass of Fuel Used (g)	Reduction in Fuel Consumption Relative to No Cylinder Disabling Values (%)	Fuel Economy (mpg)
Baseline, 1.8-litre Zetec Engine	***651.3***		***32.6***
Baseline, 1.8-litre Zetec Engine w/Cyl. Disabling	***577.6***	***11***	***36.8***
Hybrid w/Disabling, Idle the Engine	*425.0*	*13*	*50.0*
Hybrid w/Disabling, Do not Idle	*405.9*	*14*	*52.4*
Hybrid w/Disabling, No Engine Friction	*190.7*	*43*	*111.5*

As in the no disabling case, the sensitivity of the steady-state fuel economy of the vehicle with pneumatic hybridization and cylinder disabling to the air processing efficiency is of interest. Figure 3-1 shows fuel economy of the hybrid engine with cylinder disabling relative to the economy of the baseline vehicle with cylinder disabling as a function of $\eta_{a,p}$. When cylinder disabling is implemented, not using fuel during braking (with no air storage/use capabilities) results in an improvement of 19% in fuel consumption relative to the absolute baseline vehicle. The addition of idle shut off to this scheme improves fuel consumption by 27% from the baseline

value. Appendix C contains a sample of the output of the available energy analysis simulation of the hybrid internal combustion engine concept. The particular case shown corresponds to shutting off the engine at idle with the implementation of cylinder disabling.

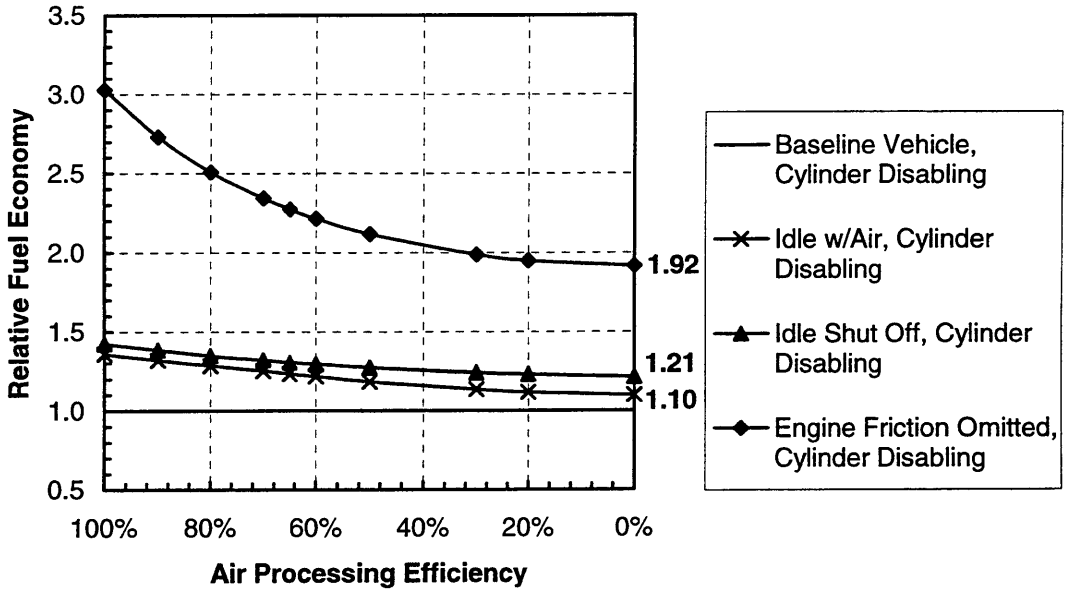

Figure 3-1. Relative Steady-State Fuel Economy vs. Air Processing Efficiency - Hybrid with Cylinder Disabling

3.3.2 Ideal Case Description and Steady-State Results

When cylinders are disabled, the friction in the non firing cylinders is less than in the firing cylinders. However, for this particular engine, we do not know by how much friction is reduced as a result of cylinder disabling. Consequently, since the results generated in Section 3.3.1 assume that engine friction does not change when disabling is used, in this section we generate results for the lowest limit of disabled cylinder friction, zero. The actual values of fuel consumption and economy lie between the results presented in these two sections. Once friction in the disabled cylinders is quantified, fuel usage can be estimated more precisely.

If the contribution to fuel flow predicted by Eq.(3.6) is ignored, the fuel consumed by the baseline engine when producing positive brake torque and engaging in ideal cylinder disabling is given by

$$\dot{m}^{*}_{f_{DSBL}} = \frac{n_{cyl}}{4} \cdot \dot{m}_{f_{best}} . \tag{3.5}$$

The mass and volume of fuel consumed by the hybrid when cylinder disabling is used are computed, respectively, via

$$\dot{m}^*_{f_{DSBL-HYBRID}} = (1-K)\times \dot{m}^*_{f_{DSBL}}$$
$$\dot{V}^*_{f_{DSBL-HYBRID}} = \frac{\dot{m}^*_{f_{DSBL-HYBRID}}}{3.785\times \rho_f} \quad . \tag{3.9}$$

In the event that the engine is absorbing torque from the transmission (the vehicle is slowing down), fuel consumption is again estimated via Eq.(2.17) or Eqs.(2.16) through (2.18), according to the description in Section 3.3.1.

Table 3-2. Results of Ideal Available Energy Analysis vs. Mode of Operation of Hybrid Internal Combustion Engine with Ideal Cylinder Disabling

Mode of Operation	Mass of Fuel Used (g)	Reduction in Fuel Consumption Relative to No Cylinder Disabling Values (%)	Fuel Economy (mpg)	Change in Fuel Consumption Relative to Real Disabling Case (%)
Baseline, 1.8-litre Zetec Engine	***651.3***		***32.6***	
Baseline, 1.8-litre Zetec Engine w/Cyl. Disabling	***446.8***	***31***	***47.6***	***-23***
Hybrid w/Disabling, Idle the Engine	*304.0*	*38*	*69.9*	*-28*
Hybrid w/Disabling, Do not Idle	*288.0*	*39*	*73.8*	*-29*
Hybrid w/Disabling, No Engine Friction	*190.7*	*43*	*111.5*	*0*

As the results on Table 3-2 show, omitting friction in the disabled cylinders in our calculations of fuel consumption and economy of the hybrid with cylinder disabling substantially overestimates the economy gain that the concept yields. Under ideal disabling conditions, the baseline vehicle yields 47.6 mpg, an improvement of 31% in fuel consumption from the no disabling case, vis a vis the improvement of 11% when friction in the non firing cylinders is assumed to be the same as in the firing cylinders. The best fuel economy attainable with hybrid performance and cylinder disabling is 73.8 mpg (when engine shut off at idle is implemented), for a reduction in fuel consumption of 56% relative to the baseline 1.8-litre Zetec engine. As expected, the values corresponding to omitting engine friction remain unchanged from the disabling case in Section 3.3.1. Reducing engine friction by 30% (in the firing cylinders, since

no friction is assumed for the disabled cylinders) brings best hybrid performance with ideal cylinder disabling fuel economy from 73.8 mpg to 78.1 mpg. The effect of engine friction on fuel consumption and economy is evident. Omitting engine friction in the cylinders that are not firing may overestimate fuel savings by as much as 29%.

The results above correspond to an air processing efficiency of 100%. Like in Sections 2.6 and 3.3.1, results of fuel economy of the hybrid internal combustion engine concept with ideal cylinder disabling in the CVS cycle were generated as a function of $\eta_{a,p}$. The values were compared to the fuel economy of the standard engine with ideal cylinder disabling, and the results are shown in Fig. 3.2. Not injecting fuel during braking (without hybrid operation) saves 39% of the fuel used by the baseline engine with no disabling. Shutting the engine off at idle results in an additional 8% savings, for a total reduction of 47% in fuel consumption from the standard engine.

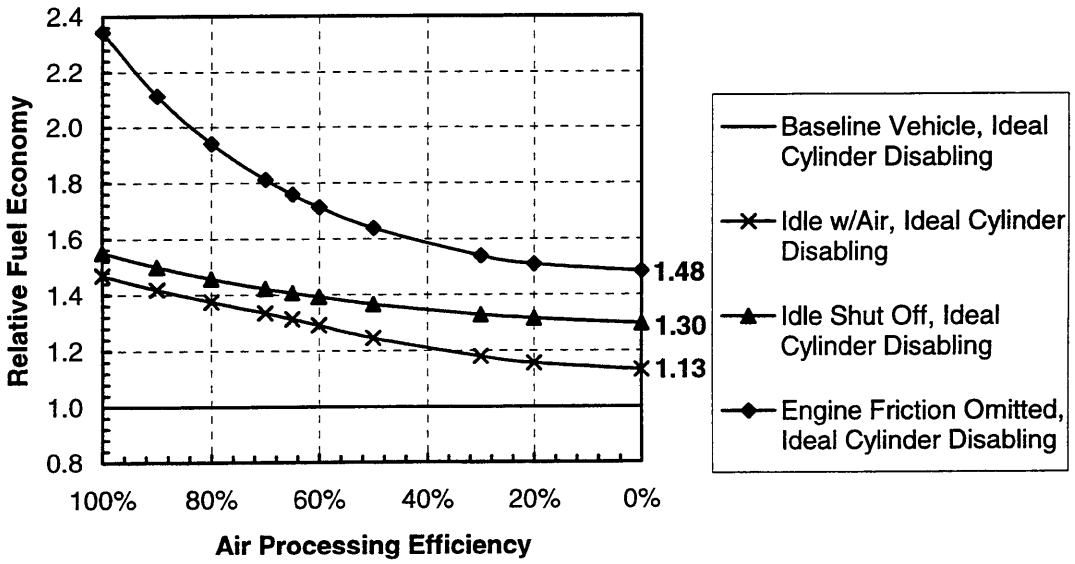

Figure 3-2. Relative Steady-State Fuel Economy vs. Air Processing Efficiency - Hybrid with Ideal Cylinder Disabling

Chapter 4 - Estimates of the Thermodynamic Irreversibilities in Hybrid Operation

4.1 Introduction

Until now, we have estimated fuel consumption and economy for the P2000 vehicle in typical urban driving for several configurations of the hybrid internal combustion engine concept. The values were computed for air processing efficiencies ranging between 100% (reversible case) and 0% (fully irreversible case). Getting more accurate figures representing how much fuel savings are attainable with the hybrid engine requires that the air compression and air expansion efficiencies be estimated. For that purpose, simple models of a braking and an air driving event were implemented. Their details are discussed in the subsequent sections.

4.2 Modeling a Typical Braking Event

The actual fluid flow and thermodynamic processes involved in a braking event in which the engine is operated as an air compressor are very complex. Air has to be inducted from the atmosphere, through the intake manifold, into the cylinders, and into the storage tank via the exhaust manifold. These processes were divided into a sequence of simpler unit events in order to estimate approximate values for the air compression efficiency as a function of several operating conditions of the hybrid, in particular the air pressure in the EM and tank.

4.2.1 Steps Involved in Braking the Vehicle

Figure 4-1 shows the physical system used in our model of a braking event. In a 4-cylinder engine, the cylinders are 180 CAD (crank angle degrees) out of phase with each other. Therefore, in this section, the hybrid engine is modeled as a single piston-cylinder device (subsystem A) connected via valve #1 (EV) to the exhaust manifold (EM, subsystem B), which in turn is connected to the air tank (subsystem C) through valve #2.

The following list describes the states and processes, together with the corresponding relations, undergone by the air involved in braking the vehicle. The actual processes are a combination of the following. In general, multi tank blowdown and mixing processes, which are extremely complex to model and analyze, are involved in a braking event. Therefore, we have assumed simplified versions of the actual thermodynamic processes.

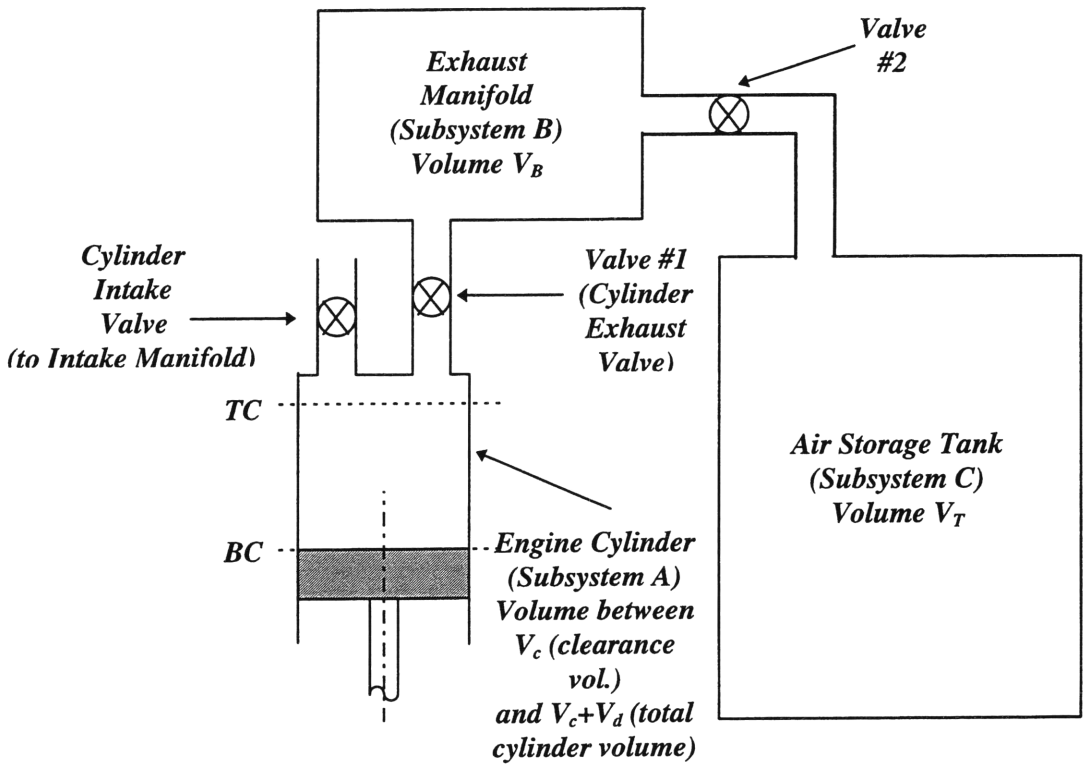

Figure 4-1. Physical System Used to Model a Braking Event

State 1:

- The piston in subsystem A is at BC ($V_{A_1} = V_c + V_d$).
- Valves #1 and #2 are closed.
- The cylinder is filled with air at atmospheric conditions.
- The exhaust manifold (subsystem B) and air tank (subsystem C) contain air at arbitrary initial conditions.

Process 1-2

The contents inside A are compressed adiabatically and reversibly to the volume required to obtain the necessary amount of braking work. This is shown in the p-V diagram in Fig. 4-2.

State 2:

- The cylinder pressure and temperature at state 2, P_{A_2} and T_{A_2} can be calculated from Eq.(D.1), where the subscripts i and f correspond to state 1 and 2, respectively.

The amount of work done in this process, $W_{1\text{-}2}$, which is equivalent to the increase in available energy of the system, is given by Eq.(D.3).

Process 2-3

Valve #1 is opened. An adiabatic instantaneous blowdown occurs between subsystems A and B (cylinder and EM). An irreversible mixing process takes place in the EM, and its contents attain a uniform temperature. Available energy is lost in this process.

State 3:

- The pressure is uniform for the contents of A and B, $P_{A_3} = P_{B_3}$, where this value is given by Eq.(D.5). The source (S) and the destination (D) tanks become subsystems A and B, respectively. The subscripts i and f correspond to states 2 and 3.
- The cylinder volume is unchanged, $V_{A_3} = V_{A_2}$.
- The temperatures inside A and B are estimated via Eqs.(D.6) and (D.9).

The loss of available energy due to this process is given by Eq.(D.10).

Process 3-3'

Valve #1 remains open. The contents of the cylinder and EM continue to be compressed isentropically by the piston until it reaches TC and the exhaust valve (EV, #1) is closed. Though gas flows into the EM, no mixing occurs.

State 3':

- Valves #1 and #2 are closed.
- The cylinder volume is $V_{A_{3'}} = V_c$.
- The new cylinder and exhaust manifold pressure is governed by Eq. (D.11).
- The temperature inside the cylinder is uniform (subsystem I), whereas there are two different temperatures inside tank B, one corresponding to the air that was transferred in process 3-3' (subsystem II) and the other one to what stayed in tank B throughout the process (subsystem III). These quantities are given by Eqs. (D.12).

The amount of work done in this process, $W_{3\text{-}3'}$, which is equivalent to the increase in available energy of the system, is given by Eq.(D.13).

Process 3'-4

The contents of the EM mix and reach a uniform temperature. Available energy is lost in this process.

State 4:

- The air pressure in the EM remains unchanged.
- The temperature of the air inside the EM is given by Eq.(D.14).

The loss of available energy resulting from this process is given by Eq.(D.15).

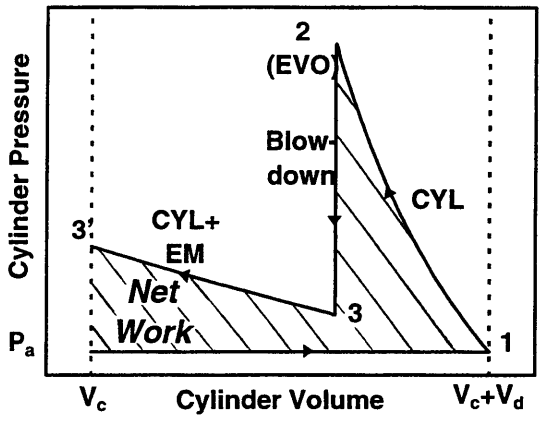

Figure 4-2. Pressure-Volume Diagram for Process 1-3' in a Braking Event

Process 4-5

Valve #2 is opened, and an adiabatic instantaneous blowdown process between the EM and the air tank takes place. An irreversible mixing process occurs in the air tank, and its contents attain a uniform temperature. Some available energy is destroyed in this process.

State 5:

- Valve #2 is closed.
- The pressure is uniform for the contents of B and C, $P_{A_5} = P_{B_5}$, where this value is given by Eq.(D.5). The source (S) and destination (D) tanks become subsystems B and C, respectively. The subscripts i and f correspond to states 4 and 5.
- The temperatures inside B and C are estimated via Eqs.(D.6) and (D.9).

The loss of available energy resulting from this process is given by Eq.(D.10).

Process 5-6

The contents of the tank lose heat to the tank walls, and available energy is lost. This process is introduced to account for the longer time constants associated with the storage of air. It is consistent with the assumption of isothermal processes used in our available energy analysis.

State 6:

- The contents of tank C are at an equilibrium pressure determined via Eq. (D.18). The temperature of the tank wall is set arbitrarily to 325 K.

As before, the loss of available energy can be obtained through Eq.(D.10).

The total braking work done per cylinder per cycle is given by the magnitude of

$$W_{1-3'} = W_{1-2} + W_{3-3'}, \tag{4.1}$$

which corresponds to the cross-hatched area in Fig. 4-2. This quantity depends on EVO timing and P_{B_2}, the pressure in the EM before EVO. In operating the hybrid engine, this parameter represents the net amount of energy per cylinder per cycle that is available from the transmission input (after accounting for engine friction) to store in the form of compressed air. From this scheme of operation, it follows that there are 2 ways to control the amount of braking done per cylinder per cycle, by controlling the timing of the exhaust valve opening (shifting state 2 in Fig. 4-2 along the volume axis), or by disabling cylinders (not allowing braking to occur in all cylinder-cycles). Ultimately, we want to maximize the air compression efficiency, and thus achieve the necessary braking while keeping the losses of available energy in the processes above to a minimum. The following section illustrates how significant blowdown, mixing, and heat losses are relative to each other, as well as how controllable they are. Furthermore, sample values of the individual losses and overall process efficiency are generated for various braking events.

4.2.2 Analysis of Losses and Braking Strategy

As this part of the operation of the hybrid internal combustion engine was analyzed, the parameter that would quantify the individual losses in a braking event in the best way was not apparent. However, after trying different approaches, we decided to express individual losses as the change in available energy of the mass of air involved in a specific process relative to the magnitude of the reversible work transfer ($W_{1-3'}$) done by the piston in the compression stroke.

The individual contributions to the overall loss of available energy in a braking event come from blowdown process 2-3, mixing process 3'-4, blowdown 4-5, and heat loss process 5-6. In terms of our definition of relative loss, we have

$$\Lambda_{2-3} = \frac{\left(W_{ava_{A_2}} - W_{ava_{A_3}}\right) + \left(W_{ava_{B_2}} - W_{ava_{B_3}}\right)}{\left|W_{1-3'}\right|}, \tag{4.2}$$

$$\Lambda_{3'-4} = \frac{W_{ava_{B_{3'}}} - W_{ava_{B_4}}}{\left|W_{1-3'}\right|}, \tag{4.3}$$

$$\Lambda_{4-5} = \frac{\left(W_{ava_{B_4}} - W_{ava_{B_5}}\right) + \left(W_{ava_{C_4}} - W_{ava_{C_5}}\right)}{\left|W_{1-3'}\right|}, \text{ and} \tag{4.4}$$

$$\Lambda_{5-6} = \frac{W_{ava_{C_5}} - W_{ava_{C_6}}}{\left|W_{1-3'}\right|}. \tag{4.5}$$

The air compression efficiency is the ratio of the available energy addition to the system to the reversible work transfer into the system. It is related to the losses via

$$\eta_{1-6} = \frac{\sum_{A,B,C} W_{ava_6} - \sum_{A,B,C} W_{ava_1}}{\left|W_{1-3'}\right|} = 1 - \Lambda_{1-6}, \tag{4.6}$$

where $\Lambda_{1\text{-}6}$ represents the sum of the Λ's given by Eqs.(4.2) through (4.5). Although efficiencies in the traditional sense are always positive, the air compression efficiency may be negative for adverse operating conditions of the hybrid engine. The physical explanation of this phenomenon is that, in attempting to store a given amount of available energy in the system, if the processes involved are highly irreversible, not only will available energy not be stored, but some of that quantity in the system will be destroyed. This is shown by the sample results generated towards the end of this section.

In order to determine the optimum valve timing strategy, the relative loss of available energy in blowdown process 2-3 was computed as a function of pre-blowdown pressure ratio for a variety of initial states. Although it is desired that the air that is inducted into the cylinder flow progressively into the EM and then into the air tank (flow is strictly from A, to B, to C), the simulation used to calculate blowdown losses allows for backflows to occur. Figures 4-3 through 4-6 show the relative loss, $\Lambda_{2\text{-}3}$, resulting from blowdown process 2-3 from the cylinder to the EM. Based on the results of our available energy analysis simulation, results were generated for EM pre-blowdown pressures (P_{B_2}) ranging between 1 atm and 16 atm. Pre-blowdown temperatures in the EM and tank were set arbitrarily. For each set of initial conditions, a family of curves was plotted in which the ratio of cylinder to EM volume was varied by factors of 2.

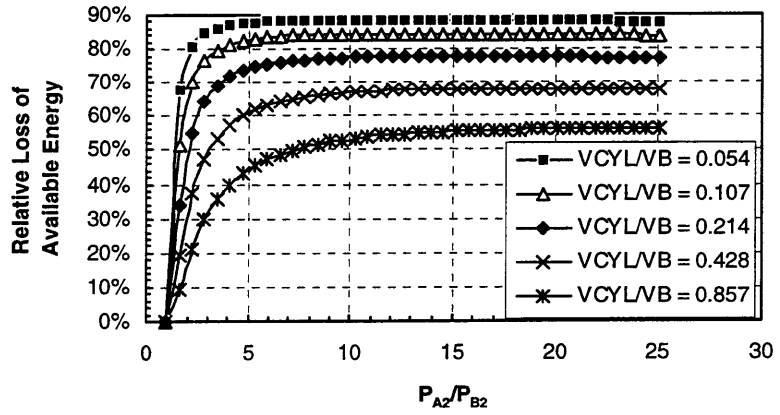

(a) $P_{B_2} = 1$ atm, $T_{B_2} = 325$ K

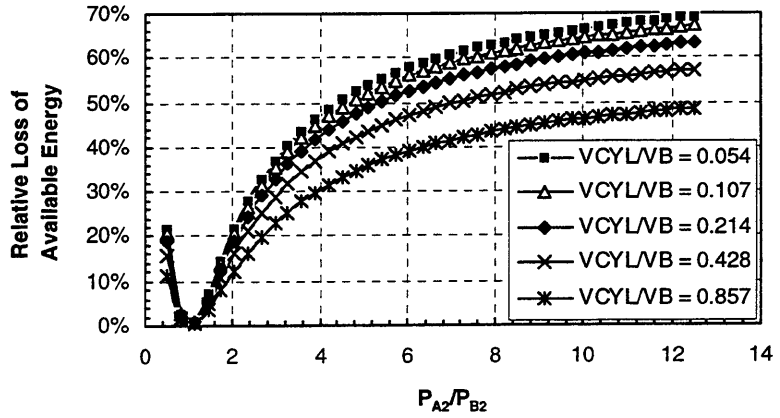

(b) $P_{B_2} = 2$ atm, $T_{B_2} = 325$ K

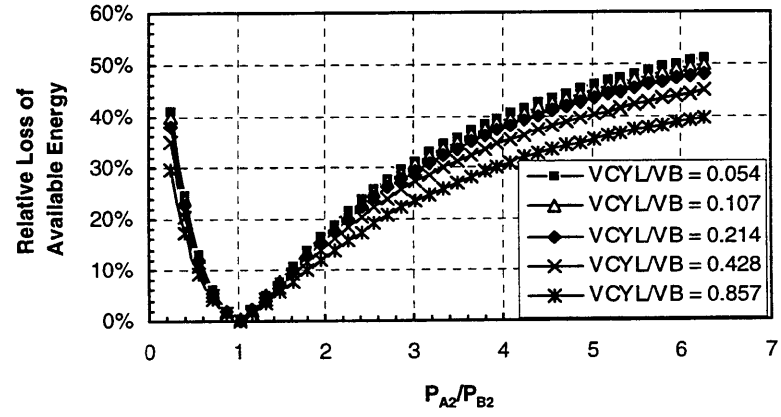

(c) $P_{B_2} = 4$ atm, $T_{B_2} = 325$ K

Figure 4-3. Relative Loss of Available Energy $\Lambda_{2\text{-}3}$ vs. Pre-Blowdown Pressure Ratio

Graphs (a), (b), and (c)

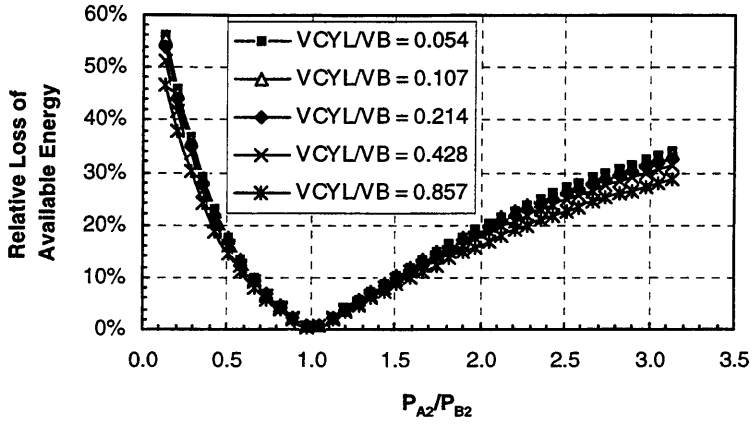

(d) $P_{B_2} = 8$ atm, $T_{B_2} = 325$ K

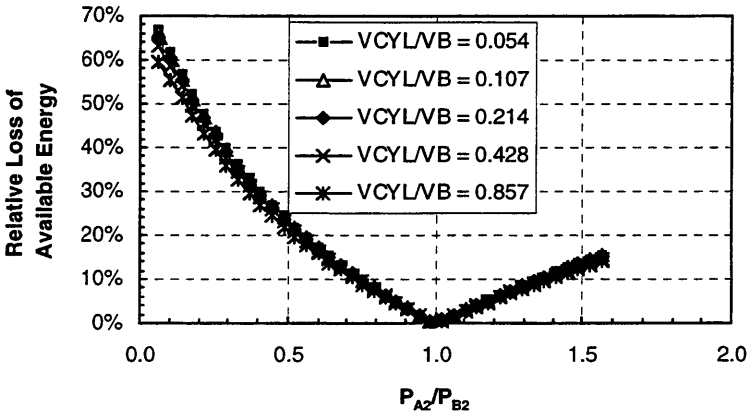

(e) $P_{B_2} = 16$ atm, $T_{B_2} = 325$ K

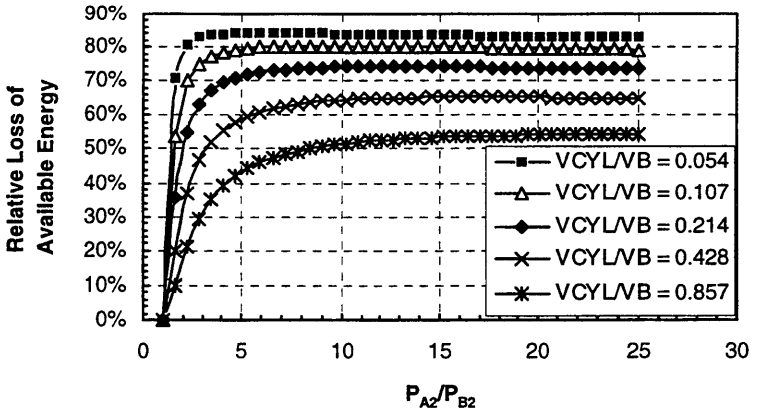

(f) $P_{B_2} = 1$ atm, $T_{B_2} = 350$ K

Figure 4-4. Relative Loss of Available Energy $\Lambda_{2\text{-}3}$ vs. Pre-Blowdown Pressure Ratio

Graphs (d), (e), and (f)

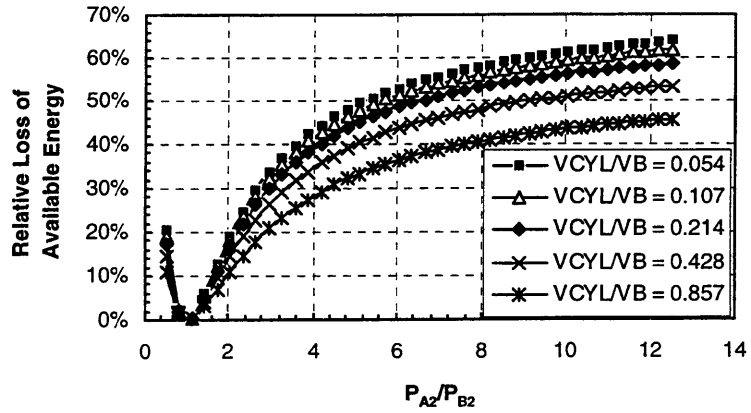

(g) $P_{B_2} = 2$ atm, $T_{B_2} = 350$ K

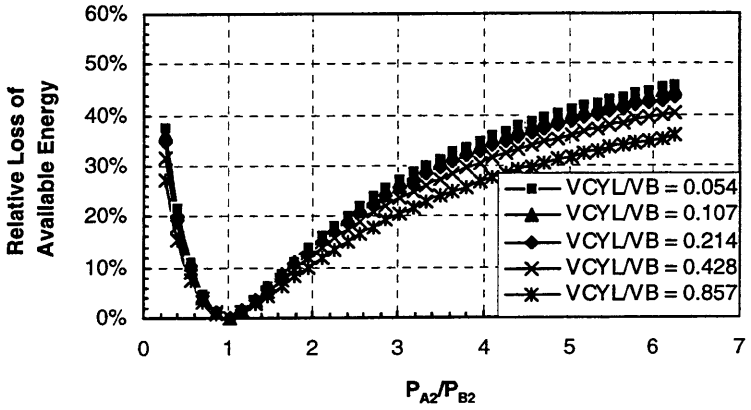

(h) $P_{B_2} = 4$ atm, $T_{B_2} = 350$ K

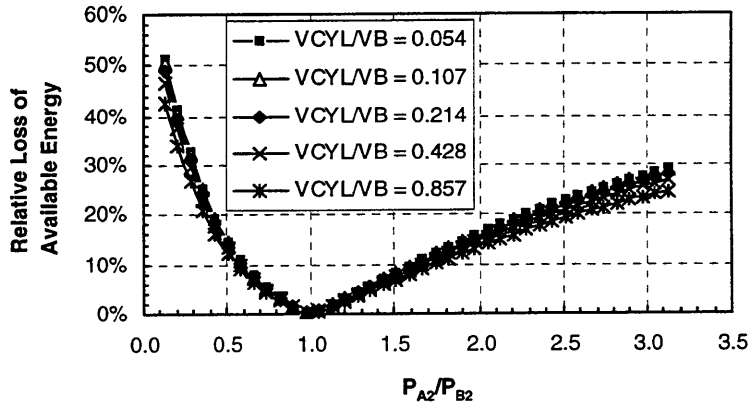

(i) $P_{B_2} = 8$ atm, $T_{B_2} = 350$ K

Figure 4-5. Relative Loss of Available Energy $\Lambda_{2\text{-}3}$ vs. Pre-Blowdown Pressure Ratio

Graphs (g), (h), and (i)

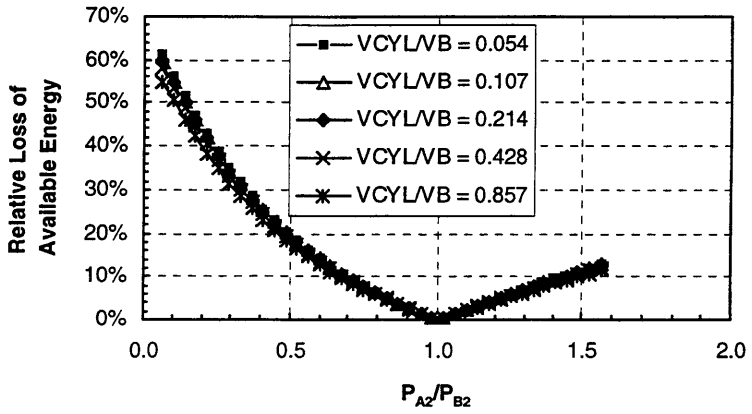

(j) $P_{B_2} = 16$ atm, $T_{B_2} = 350$ K

Figure 4-6. Relative Loss of Available Energy $\Lambda_{2\text{-}3}$ vs. Pre-Blowdown Pressure Ratio

Graph (j)

The graphs in Figs. 4-3 through 4-6 illustrate several points. The first thing that can be observed when comparing the sets of graphs for two different pre-blowdown EM temperatures, 325 K and 350 K, is that the relative blowdown loss in process 2-3 and that quantity are inversely related. However, examining the numbers closely shows that the difference in losses for both cases is not significant. The parameters that the relative loss $\Lambda_{2\text{-}3}$ is most sensitive to are the pre-blowdown pressure P_{B_2} and the pressure ratio P_{A_2}/P_{B_2}.

When the initial pressure in the EM is 1 atm, graphs (a) and (f) show that it is impossible to fulfill the braking requirements of the CVS cycle while maintaining the relative loss of available energy resulting from process 2-3 at a low level. Although the cylinder to manifold pressure ratio at state 2 can be maintained at a small value, below 1.1 for example, to obtain a small loss, the magnitude of the braking work done under these conditions is much smaller than the typical value of 58 J/cylinder-cycle.

In the case that P_{B_2} is in the range of 4 atm or higher, the situation is more favorable: highly dissipative blowdown processes may be avoided while achieving enough braking by compressing air in the engine cylinders. Maintaining P_{A_2}/P_{B_2} below 2 guarantees a relative loss $\Lambda_{2\text{-}3}$ of less than 20%. As P_{B_2} increases, the value of the ratio corresponding to the 20% loss also grows. This fact has favorable implications, since as P_{B_2} and P_{A_2}/P_{B_2} increase, the amount of

braking work that is done per cylinder in each stroke, $W_{1\text{-}3'}$, is augmented. Consequently, as the pressure in the EM at EVO timing (state 2) increases, achieving the required amount of braking work dissipates less available energy in a relative sense.

The relative loss in a blowdown process is also dependent on the ratio of the volumes involved. The nominal values used for Figs. 4-3 through 4-6 are, for the total cylinder volume, $V_{CYL} = V_c + V_d$ =49.92 cm^3 + 449.00 cm^3 = 498.92 cm^3, and for the exhaust manifold, V_{EM} = 2,330 cm^3. As the source to destination volume ratio (cylinder to EM in this case) increases, the relative loss decreases for given values of P_{B_2} and P_{A_2}/P_{B_2}. However, the volume ratio only has a substantial effect (10 %) in the reduction of the loss when P_{B_2} is small (1 atm and 2 atm) and the pre-blowdown pressure ratio is larger than 2. When the pressure in the EM at state 2 is higher, the effects of changes in volume ratio by a factor of at most 4 are not significant, as Figures 4-3 through 4-6 show. Increasing the volume of the exhaust manifold would reduce the loss due to process 2-3 slightly, but would increase that resulting from blowdown process 4-5. When blowdown processes are involved, the optimum scenario is when the source tank is much larger (> 30 times) than the destination. This makes the relative loss of available energy insignificant.

Tables 4-1 and 4-2 show values for the individual losses involved in a braking event as a function of pre-blowdown pressure ratios and EM and tank pressures. These results assume temperatures $T_{B_2} = 350$ K and $T_{C_4} = T_{C_6} = 325$ K (equilibrium tank temperature). Exhaust valve opening timing is adjusted so that the net amount of braking work has a magnitude of 58 J/cylinder-cycle, the average value obtained from the CVS cycle simulation. However, as the pressure in the exhaust manifold at state 2 increases, this amount of work may not be attainable due to the higher cylinder and EM pressure. For those cases, when P_{B_2} is 4 atm or higher, EVO timing is chosen such that the braking work done per cylinder-cycle is as close to the average value as possible (on the high side). This happens when $P_{A_2} = P_{B_2}$, which results in process 2-3 being loss free, since no unrestrained expansion occurs.

The tank pressure before blowdown process 4-5, P_{C_4}, is varied between 1 atm, 2 atm, 4 atm, and 8 atm for each case, and flow of air is allowed only from the EM into the tank. This is done to determine how sensitive the air compression efficiency is to the relative loss from process 4-5. The rows in tables 4-1 and 4-2 contain the net braking work done per cylinder-cycle, the EVO timing in degrees after bottom center (BC), the relative losses involved

in each individual process, the total relative loss for the braking event, and the air compression efficiency for each set of initial conditions. These results dictate what the operation strategy of the hybrid internal combustion engine must be in braking mode. The key to obtaining high air compression efficiencies lies in minimizing blowdown processes from the cylinder to the EM while providing enough braking work, and in maintaining the pre-blowdown pressure ratio between the EM and the tank below the range 1.15-1.20.

Table 4-1. Relative Loss of Available Energy in Various Braking Events

Pre -Blowdown Conditions	$P_{B_2} = 1\ atm$ $P_{C_4} = 1\ atm$ $\frac{P_{A_2}}{P_{B_2}} = 6.9$ $\frac{P_{B_4}}{P_{C_4}} = 1.4$	$P_{B_2} = 2\ atm$ $P_{C_4} = 2\ atm$ $\frac{P_{A_2}}{P_{B_2}} = 2.9$ $\frac{P_{B_4}}{P_{C_4}} = 1.2$	$P_{B_2} = 2\ atm$ $P_{C_4} = 1\ atm$ $\frac{P_{A_2}}{P_{B_2}} = 2.9$ $\frac{P_{B_4}}{P_{C_4}} = 2.3$	$P_{B_2} = 4\ atm$ $P_{C_4} = 4\ atm$ $\frac{P_{A_2}}{P_{B_2}} = 1.0$ $\frac{P_{B_4}}{P_{C_4}} = 1.1$	$P_{B_2} = 4\ atm$ $P_{C_4} = 2\ atm$ $\frac{P_{A_2}}{P_{B_2}} = 1.0$ $\frac{P_{B_4}}{P_{C_4}} = 2.2$
$W_{1\text{-}3'}$ (J/cyl-cycle)	*-57.9*	*-57.9*	*-57.9*	*-72.9*	*-72.9*
EVO (deg. ABC)	*137*	*132*	*132*	*121*	*121*
IRREVERSIBLE PROCESS	***RELATIVE LOSS OF AVAILABLE ENERGY***				
2-3	*73.2%*	*28.9%*	*28.9%*	*0.00%*	*0.00%*
3'-4	*0.83%*	*0.04%*	*0.04%*	*5.2%*	*5.2%*
4-5	*16.0%*	*8.1%*	*160.4%*	*3.4%*	*201.6%*
5-6	*10.7%*	*9.4%*	*33.5%*	*6.9%*	*43.9%*
TOTAL RELATIVE LOSS	*100.7%*	*46.5%*	*222.8%*	*15.5%*	*250.7%*
AIR COMPRESSION EFFICIENCY	*-0.71%*	*53.5%*	*-122.8%*	*84.5%*	*-150.7%*

Fulfilling the braking demand of the CVS cycle and keeping the loss from process 2-3 to a minimum requires a pre-blowdown EM pressure of at least 4 atm. When this is the case, tables 4-1 and 4-2 show that the amount of braking work done per cylinder-cycle may exceed the necessary amount. In that case, we choose to open valve #1 (EV) when the pressure in the cylinder is equivalent to that in the EM. There are no blowdown losses between A and B, and the amount of braking is controlled by disabling cylinders. The high pre-blowdown EM pressure can be attained by maintaining the air tank above a certain pressure level, 4 atm as suggested by Moyer, and using it to fill the manifold before braking commences. This method would perform well, since the blowdown process from C to B is not significantly dissipative due to the large source to destination volume ratio (approximately 34). If the EM is initially at atmospheric

pressure, a typical braking event of 58 J/cylinder-cycle charges it to 2 atm in 5 cylinder-cycles and to 4 atm in 15 cylinder-cycles, taking 0.06 sec and 0.17 sec to do so, respectively, assuming that all 4 engine cylinders are used in each cycle and that there is one braking cycle per revolution (2-stroke operation).

Table 4-2. Relative Loss of Available Energy in Various Braking Events

Pre -Blowdown Conditions	$P_{B_2} = 4\ atm$ $P_{C_4} = 1\ atm$ $\frac{P_{A_2}}{P_{B_2}} = 1.0$ $\frac{P_{B_4}}{P_{C_4}} = 4.3$	$P_{B_2} = 8\ atm$ $P_{C_4} = 8\ atm$ $\frac{P_{A_2}}{P_{B_2}} = 1.0$ $\frac{P_{B_4}}{P_{C_4}} = 1.04$	$P_{B_2} = 8\ atm$ $P_{C_4} = 4\ atm$ $\frac{P_{A_2}}{P_{B_2}} = 1.0$ $\frac{P_{B_4}}{P_{C_4}} = 2.1$	$P_{B_2} = 8\ atm$ $P_{C_4} = 2\ atm$ $\frac{P_{A_2}}{P_{B_2}} = 1.0$ $\frac{P_{B_4}}{P_{C_4}} = 4.2$	$P_{B_2} = 8\ atm$ $P_{C_4} = 1\ atm$ $\frac{P_{A_2}}{P_{B_2}} = 1.0$ $\frac{P_{B_4}}{P_{C_4}} = 8.3$
$W_{1\text{-}3'}$ (J/cyl-cycle)	*-72.9*	*-109*	*-109*	*-109*	*-109*
EVO (deg. ABC)	*121*	*141*	*141*	*141*	*141*
IRREVERSIBLE PROCESS	***RELATIVE LOSS OF AVAILABLE ENERGY***				
2-3	*0.00%*	*0.00%*	*0.00%*	*0.00%*	*0.00%*
3'-4	*5.2%*	*9.7%*	*9.7%*	*9.7%*	*9.7%*
4-5	*630.6%*	*1.2%*	*237.6%*	*785.5%*	*1510%*
5-6	*56.4%*	*4.2%*	*52.8%*	*68.6%*	*72.8%*
TOTAL RELATIVE LOSS	*692.3%*	*15.1%*	*300.1%*	*863.8%*	*1593%*
AIR COMPRESSION EFFICIENCY	*-592.3%*	*84.9%*	*-200.1%*	*-763.8%*	*-1493%*

Control of the blowdown process between the exhaust manifold and the air tank depends on the opening timing of valve #2. There is additional freedom in the operation of this valve than there is in that of valve #1, since the former is not used to control braking work. Optimum operation of valve #2 requires that it be opened (and left open) when the pressure in the EM reaches that in the tank. Modeling the corresponding processes entails a merger of 3 tanks which makes the analysis more complex. Since our model deals with at most 2 tanks connected simultaneously, we choose to open the connection between the EM and the tank as frequently as needed to maintain the pressure ratio P_{B_4}/P_{C_4} within the limits described above, thus keeping the loss from process 4-5 as low as allowable.

The mixing and heat transfer contributions (from processes 3'-4 and 5-6, respectively) to total relative loss are not directly controllable. Their magnitudes depend on the initial and equilibrium temperatures assumed. Furthermore, these losses are related to the outcome of the blowdown processes. As the opening timing of valve #1 shifts closer to TC, the mixing process (3'-4) becomes less dissipative, since the mass of air that mixes in this process is transferred from the cylinder to the EM as the piston travels from the EVO point to TC. Similarly, the loss of available energy resulting from process 5-6 is directly related to the amount of mass transferred from the EM into the tank in process 4-5. It is also sensitive to the assumed equilibrium temperature, T_{C_6}.

In conclusion, optimum operation of the hybrid internal combustion engine in braking mode requires that the pressure inside the air tank be always maintained at a pressure no less than 4 atm. Before braking commences, the EM is charged with air from the tank, and the connection between the EM and the storage tank is left open. The exhaust valve of the cylinder is opened when the cylinder pressure reaches that in the EM, and it remains open until the piston reaches TC. As the compression stroke is completed in each cylinder, the pressure of the EM and tank rises, and thus EVO timing occurs later in the compression stroke for the subsequent cylinders. When the net amount of braking work done exceeds the per cylinder-cycle work requirement, cylinders are disabled. Fully variable valve timing and cylinder disabling are essential in minimizing thermodynamic losses in air storage and in controlling the amount of braking work done to fulfill the braking requirements of the CVS cycle.

If this strategy is followed (with the limitation in our model that no more than 2 tanks may be connected at a time), our calculations predict an air compression efficiency no lower than 84.5%. However, as we pointed out above, this result is sensitive to assumptions about initial temperatures. Furthermore, since our model is not exact, the actual efficiency is likely to be smaller. For these reasons, and to be consistent with the air driving case, we conclude that 65%, as predicted in Chapter 2, is a suitable value for the overall air compression efficiency.

4.3 Modeling a Typical Air Driving Event

As in the braking case, the fluid flow processes involved in driving the vehicle on compressed air are complex. There are two possible ways to operate the hybrid internal combustion engine in air driving mode. Air can flow from the storage tank into the IM, to the engine cylinders, and out to the atmosphere via the EM and catalytic converter. This poses a problem, since air flow through the catalyst will cool it down, dropping its efficiencies and

increasing tailpipe emissions. The alternative is to operate the exhaust manifold as intake and the cylinders' exhaust valves as intake. This reduces the problem above to having stationary gas in the catalyst. Furthermore, it allows for a simpler system, since no connection between the tank and the IM is required. Most importantly, this configuration allows for better use of the compressed air. Whenever there is enough air in storage to use for driving, it is because a braking event in which compressed air is stored has just concluded. At this point, there is pressurized air in the EM which may be used to drive the vehicle. If the former means of operation were used, this air would have to be vented to the atmosphere, wasting all its available energy.

In this section, the processes that compressed air undergoes to power the vehicle are simplified into a set of unit processes with known outcomes. As in a braking event, this is done to avoid dealing with complex models of the real processes. This then allows us to estimate a range of values for the air expansion efficiency. The calculation is run for several initial tank pressures above 4 atm, the minimum established in the previous section, and for a variety of initial "IM"[1] conditions.

4.3.1 Steps Involved in Driving the Vehicle on Compressed Air

Since we chose to use the EM as intake during an air driving event, the diagram in Fig. 4-1 is applicable to our analysis of the hybrid internal combustion engine in air driving mode. Subsystems A, B, and C are the cylinder, EM, and air tank, respectively, as before. The following list describes the states and processes, together with the corresponding relations, that the pressurized air used to drive the vehicle undergoes. The p-V diagram in Fig. 4-7 shows this sequence of steps.

State 1:

- The piston in subsystem A is at TC ($V_{A_1} = V_c$).
- Valves #1 and #2 are closed.
- The cylinder contains air at atmospheric pressure..
- The temperature of the air in the cylinder at this state is the same as that at state 8 described below. Calculating its value is an iterative process.

[1] "IM" refers to the exhaust manifold behaving as the intake manifold. The same applies to "IV" vs. EV (cylinder exhaust valve).

- The exhaust manifold (subsystem B) and air tank (subsystem C) contain air at initial conditions determined using the knowledge gained from the braking event, since air driving follows braking.

Process 1-2

Valve #2 is opened. An adiabatic instantaneous blowdown occurs between subsystem C and subsystem B (air storage tank and EM). An irreversible mixing process takes place in the EM, and its contents attain a uniform temperature. Available energy is lost in this process.

State 2:

- Valve # is closed.
- The pressure is uniform for the contents of B and C, $P_{B_2} = P_{C_2}$, where this value is given by Eq.(D.5). The source (*S*) and the destination (*D*) tanks become subsystems C and B, respectively. The subscripts *i* and *f* correspond to states 1 and 2.
- The state of the air inside the cylinder is unchanged.
- The temperatures inside B and C are estimated via Eqs.(D.9) and (D.6), respectively.

The loss of available energy due to this process is given by Eq.(D.10).

Process 2-3

Valve #1 ("IV") is opened. An adiabatic instantaneous blowdown process takes place between subsystem B and subsystem A (EM and cylinder at TC). An irreversible mixing process takes place within the cylinder, and its contents attain a uniform temperature. Available energy is lost in this process.

State 3:

- The pressure is uniform for the contents of A and B, $P_{A_3} = P_{B_3}$, where this value is given by Eq.(D.5). The source (*S*) and the destination (*D*) tanks represent subsystems B and A, respectively. The subscripts *i* and *f* correspond to states 2 and 3.
- The cylinder volume is unchanged. The piston remains at TC.
- The temperatures inside A and B are estimated via Eqs.(D.9) and (D.6).

The loss of available energy resulting from this blowdown is estimated through Eq.(D.10).

Process 3-3'

Valve #1 ("IV") remains open, and the contents of the cylinder and EM are expanded adiabatically and reversibly all the way to valve #1 closing ("IVC"). Although gas flows into the cylinder, no mixing occurs.

State 3':

- Valve #1 is closed.
- The cylinder volume, chosen as a function of the amount of driving work needed, is $V_{A_{3'}}$.
- The new cylinder and exhaust manifold pressure is governed by Eq. (D.11).
- The temperature inside the EM is uniform (subsystem I). However, there are two different temperatures inside the cylinder (A), one corresponding to the air that was transferred in process 3-3' (subsystem II) and the other one to what stayed in A throughout the process (subsystem III). These quantities are given by Eqs. (D.12).

The amount of work done by the air in this process, $W_{3\text{-}3'}$, which is equivalent to the reduction in available energy of the system, is given by Eq.(D.13).

Process 3'-4

The contents of the cylinder mix and reach a uniform temperature. Available energy is lost in this process.

State 4:

- The cylinder volume remains unchanged, $V_{A_4} = V_{A_{3'}}$.
- The cylinder pressure does not change.
- The cylinder temperature is given by Eq.(D.14).

The loss of available energy resulting from this process is given by Eq.(D.15).

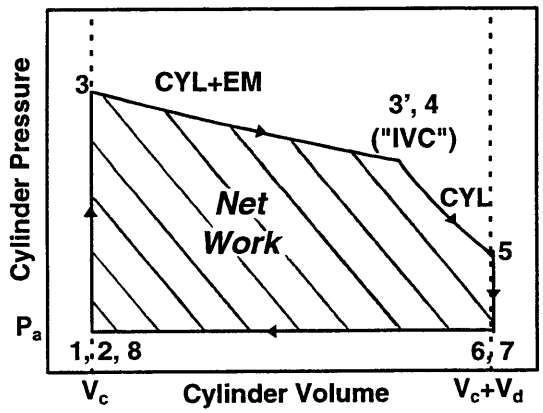

Figure 4-7. Pressure-Volume Diagram for an Air Driving Event

Process 4-5

The contents of the cylinder, now at a uniform temperature, expand isentropically until the piston reaches BC.

State 5:

- At BC, the cylinder volume is $V_{A_5} = V_c + V_d$, the full volume.
- The cylinder pressure and temperature at state 5, P_{A_5} and T_{A_5} can be calculated from Eq.(D.1), where the subscripts i and f correspond to state 4 and 5, respectively.

The amount of work done by the air on the piston in this process, $W_{4\text{-}5}$, which is equivalent to the decrease in available energy of the system, is given by Eq.(D.3).

Process 5-6

The cylinder's intake valve, operating as exhaust, is opened. If the cylinder pressure at state 5 is greater than atmospheric, some air is blown out into the IM ("EM"), and available energy is lost in the process. On the other hand, if the pressure at BC is sub-atmospheric, air flows into the cylinder, and available energy is also lost.

State 6:

- The cylinder pressure at state 6 is $P_{A_6} = P_a$.
- The cylinder temperature at state 6 is given by Eq.(D.20) or (D.20) and (D.21), depending upon the cylinder pressure at state 5.

Process 6-7

The contents of the tank absorb heat from the tank walls, and some available energy is gained. This process is analogous to heat loss process 5-6 involved in a braking event.

State 7:

- The contents of tank C are at an equilibrium pressure determined via Eq. (D.18). The temperature of the tank wall is set arbitrarily to 325 K.

As before, the negative loss (gain) of available energy can be obtained through Eq.(D.10).

Process 7-8

The piston travels back to TC for the next cycle. Some air (and thus available energy) is pushed out of the cylinder.

State 8:

- "EV" is closed.
- The cylinder pressure and temperature remain at their values from state 6.
- The mass remaining in the cylinder is calculated via Eq.(D.22).

The total net driving work done per cylinder per cycle is given by

$$W_{3-5} = W_{3-3'} + W_{4-5}, \tag{4.7}$$

which corresponds to the cross-hatched area in Fig. 4-7. This quantity depends on "IVC" timing and P_{B_2}, the pressure in the EM before "IVO". After deducting friction power from this value, we obtain the amount of power that the engine crankshaft can transmit to the transmission input. The amount of driving work done is controllable by adjusting the timing of the "intake valve" opening and by implementing cylinder disabling. Our goal is to provide the amount of energy needed to drive the vehicle while keeping the loss of available energy at a minimum level, maximizing the air expansion efficiency. The following section contains sample values of the individual losses involved in typical accelerating events. Furthermore, values for the expansion efficiency are also estimated.

4.3.2 Analysis of Losses and Air Driving Strategy

Several of the thermodynamic processes involved in an air driving event are similar to those in a braking event. When operating in this mode, extracting an amount of energy $W_{3\text{-}5}$ from the whole system in a cycle entails a reduction in the available energy of the system that is at least as large as the reversible work transfer above. Consequently, losses are measured as the drop in available energy resulting from a specific process relative to the decrease in the available energy of the system as it goes from state 1 to state 8.

Available energy is lost in blowdown processes 1-2 and 2-3, mixing process 3'-4, blowdown process 5-6, and in constant pressure and temperature process 7-8. Some available energy is gained in process 6-7 as the contents of the air tank absorb heat from the tank wall. This is denoted as a negative loss. In terms of this definition of relative loss, we have

$$\Phi_{1-2} = \frac{\left(W_{ava_{B_1}} - W_{ava_{B_2}}\right) + \left(W_{ava_{C_1}} - W_{ava_{C_2}}\right)}{\sum_{A,B,C} W_{ava_1} - \sum_{A,B,C} W_{ava_8}}, \tag{4.8}$$

$$\Phi_{2-3} = \frac{\left(W_{ava_{B_2}} - W_{ava_{B_3}}\right) + \left(W_{ava_{A_2}} - W_{ava_{A_3}}\right)}{\sum_{A,B,C} W_{ava_1} - \sum_{A,B,C} W_{ava_8}}, \tag{4.9}$$

$$\Phi_{3'-4} = \frac{W_{ava_{A_{3'}}} - W_{ava_{A_4}}}{\sum_{A,B,C} W_{ava_1} - \sum_{A,B,C} W_{ava_8}}, \tag{4.10}$$

$$\Phi_{5-6} = \frac{W_{ava_{A_5}} - W_{ava_{A_6}}}{\sum_{A,B,C} W_{ava_1} - \sum_{A,B,C} W_{ava_8}}, \tag{4.11}$$

$$\Phi_{6-7} = \frac{W_{ava_{C_6}} - W_{ava_{C_7}}}{\sum_{A,B,C} W_{ava_1} - \sum_{A,B,C} W_{ava_8}}, \text{ and} \tag{4.12}$$

$$\Phi_{7-8} = \frac{W_{ava_{A_7}} - W_{ava_{A_8}}}{\sum_{A,B,C} W_{ava_1} - \sum_{A,B,C} W_{ava_8}}. \tag{4.13}$$

The air expansion efficiency is the ratio of the amount of work obtained from the system to the total reduction in its available energy as the work is extracted. It is given by

$$\eta_{a,e} = \frac{W_{3-5}}{\sum_{A,B,C} W_{ava_1} - \sum_{A,B,C} W_{ava_8}} = 1 - \Phi_{1-8}, \tag{4.14}$$

where $\Phi_{1\text{-}8}$ represents the sum of the Φ's given above.

The analysis on 2-tank blowdown processes carried out in Section 4.2.2 carries over to air driving events. The unrestrained expansion between the "IM" (EM) and the clearance volume of the cylinder (process 2-3) does not have a significant effect on the air expansion efficiency, since the ratio of source to destination volume is approximately 46. The results of our analysis of the hybrid system show that the process that determines the overall level of irreversibility in a driving event is blowdown/tank filling process 5-6. Specifically, the cylinder pressure at the end of expansion, P_{A_5}, which is a function of the cylinder pressure at the beginning of the stroke, P_{A_3}, and of "IVC" timing, has much control of the value of the air expansion efficiency. The cylinder pressure at TC and "IVC" timing, in turn, control the reversible work transfer $W_{3\text{-}5}$.

Since we decided to maintain the air pressure in the tank at no less than 4 atm, the simulation of an air driving event was run for initial tank pressures of 4 atm and 8 atm. Initial EM pressures used were 4 atm and 3 atm, for the former case, and 8 atm and 6 atm for the latter. The pre-blowdown pressure ratio P_{C_1}/P_{B_1} is either 1.0 or 1.3. In the operation of the hybrid engine in air driving mode, the value of the ratio above is 1.0 during the first engine cycle, since air driving commences immediately after braking mode ends. If the tank and EM are disconnected for the remainder of the driving stroke (as our model requires), and reconnected in the next engine cycle (which minimizes the loss of available energy resulting from process 1-2), the maximum possible reduction in EM pressure, occurring when the combined contents of the

EM and cylinder are expanded for a full cylinder stroke is given, for a reversible adiabatic expansion, by a factor

$$\left(\frac{V_c + V_d + V_B}{V_c + V_B}\right)^{\gamma} = \left(1 + \frac{V_d}{V_c + V_B}\right)^{\gamma} \approx 1.27, \tag{4.15}$$

which is within the range used in our calculation.

Tables 4-3 through 4-6 contain values for the relative loss of available energy in each step of an air driving event for several sets of operating conditions described above. Values for the net driving work done per cylinder-cycle are also shown. "IVC" timing, in degrees after top center, and cylinder pressure at the end of expansion, P_{A_5}, are monitored for each set of conditions. The results assume an initial EM temperature T_{B_1} of 350 K, as well as a tank initial and equilibrium temperature $T_{C_1} = T_{C_7} = 325$ K.

Table 4-3. Relative Loss of Available Energy in Various Air Driving Events

Pre -Blowdown Conditions $P_{C_1} = 4\ atm$, $\frac{P_{C_1}}{P_{B_1}} = 1.0$	$\frac{P_{B_2}}{P_{A_2}} = 4.0$	$\frac{P_{B_2}}{P_{A_2}} = 4.0$	$\frac{P_{B_2}}{P_{A_2}} = 4.0$	$\frac{P_{B_2}}{P_{A_2}} = 4.0$
$W_{3\text{-}5}$ *(J/cyl-cycle)*	*52.3*	*67.6*	*103.1*	*-15.5*
"IVC" (deg. ATC)	*53*	*63*	*99*	*0*
Pressure P_{A_5} *(atm)*	*0.76*	*1.0*	*2.0*	*0.16*
IRREVERSIBLE PROCESS	***RELATIVE LOSS OF AVAILABLE ENERGY***			
1-2	*0.00%*	*0.00%*	*0.00%*	*0.00%*
2-3	*8.3%*	*6.8%*	*4.1%*	*41.5%*
3'-4	*0.51%*	*0.32%*	*0.20%*	*0.00%*
5-6	*3.1%*	*0.00%*	*12.6%*	*167.1%*
6-7	*0.00%*	*0.00%*	*0.00%*	*0.00%*
7-8	*3.8%*	*5.4%*	*3.6%*	*10.9%*
TOTAL RELATIVE LOSS	*15.7%*	*12.5%*	*20.5%*	*219.5%*
AIR EXPANSION EFFICIENCY	*84.3%*	*87.5%*	*79.5%*	*-119.5%*

Within each table, results are shown for 4 different exhaust valve (operating as intake) closing timings. These correspond to a net driving work of 52 J/cylinder-cycle required for an

average acceleration, to cylinder pressures at BC of 1 atm (no blowdown/tank filling process 5-6 takes place) and 2 atm, and to "IVC" occurring at TC (there is no mixing process 3'-4). The values obtained show that, for a given set of initial pressure conditions in the tank and EM, the best performance of the system is obtained when "IVC" is controlled so that the cylinder pressure at the end of the expansion stroke is 1 atm. This eliminates process 5-6 from the sequence.

Table 4-4. Relative Loss of Available Energy in Various Air Driving Events

Pre -Blowdown Conditions $P_{C_1} = 4\ atm$ $\frac{P_{C_1}}{P_{B_1}} = 1.33$	$\frac{P_{B_2}}{P_{A_2}} = 3.97$	$\frac{P_{B_2}}{P_{A_2}} = 3.97$	$\frac{P_{B_2}}{P_{A_2}} = 3.97$	$\frac{P_{B_2}}{P_{A_2}} = 3.97$
$W_{3\text{-}5}$ *(J/cyl-cycle)*	*52.3*	*67.2*	*102.4*	*-15.7*
"IVC" (deg. ATC)	*53*	*63*	*100*	*0*
Pressure P_{A_5} *(atm)*	*0.76*	*1.0*	*2.0*	*0.16*
IRREVERSIBLE PROCESS	***RELATIVE LOSS OF AVAILABLE ENERGY***			
1-2	*33.4%*	*27.8%*	*17.5%*	*100.9%*
2-3	*6.8%*	*5.7%*	*3.6%*	*20.8%*
3'-4	*0.38%*	*0.26%*	*0.17%*	*0.00%*
5-6	*2.14%*	*0.00%*	*10.9%*	*90.5%*
6-7	*-17.4%*	*-14.5%*	*-9.1%*	*-52.3%*
7-8	*1.6%*	*2.4%*	*1.8%*	*7.1%*
TOTAL RELATIVE LOSS	*26.8%*	*21.7%*	*24.8%*	*166.9%*
AIR EXPANSION EFFICIENCY	*73.2%*	*78.3%*	*75.2%*	*-66.1%*

When P_{A_5} is not 1 atm, calculations show that if it is above atmospheric level, so that process 5-6 is a blowdown, the estimates for the air expansion efficiency are higher than when it is sub-atmospheric, which makes step 5-6 a tank filling process, as described in Appendix D. As the cylinder pressure at the end of expansion drops below 1 atm, the efficiency decreases gradually, since the increased pressure difference $P_a - P_{A_5}$ augments the loss of available energy in process 5-6, and there is a decline in the net expansion work $W_{3\text{-}5}$. Consequently, their ratio descends dramatically. In fact, Tables 4-3 and 4-4 also show that, for some combinations of initial tank pressure and very low values of P_{A_5}, 4 atm and 0.16 atm, respectively, in this case,

the efficiency can turn negative. This is because, whenever there is sub-atmospheric pressure in the cylinder and the piston is displaced, a net amount of negative work is done. Instead of cylinder air doing work on the piston, the converse takes place. Specific combinations of cylinder pressure at TC and "IVC" timing may result in the negative portion of work to exceed the positive contribution, making $W_{3\text{-}5}$, and thus the air expansion efficiency, negative.

Table 4-5. Relative Loss of Available Energy in Various Air Driving Events

Pre -Blowdown Conditions $P_{C_1} = 8\ atm$, $\frac{P_{C_1}}{P_{B_1}} = 1.0$	$\frac{P_{B_2}}{P_{A_2}} = 8.0$	$\frac{P_{B_2}}{P_{A_2}} = 8.0$	$\frac{P_{B_2}}{P_{A_2}} = 8.0$	$\frac{P_{B_2}}{P_{A_2}} = 8.0$
$W_{3\text{-}5}$ *(J/cyl-cycle)*	*52.3*	*106*	*180*	*14.4*
"IVC" (deg. ATC)	*24*	*40*	*63*	*0*
Pressure P_{A_5} *(atm)*	*0.54*	*1.0*	*2.0*	*0.31*
IRREVERSIBLE PROCESS	***RELATIVE LOSS OF AVAILABLE ENERGY***			
1-2	*0.00%*	*0.00%*	*0.00%*	*0.00%*
2-3	*20.1%*	*11.8%*	*6.8%*	*36.3%*
3'-4	*1.1%*	*0.73%*	*0.50%*	*0.00%*
5-6	*9.6%*	*0.00%*	*10.3%*	*31.8%*
6-7	*0.00%*	*0.00%*	*0.00%*	*0.00%*
7-8	*3.5%*	*9.9%*	*6.8%*	*0.03%*
TOTAL RELATIVE LOSS	*34.3%*	*22.4%*	*24.5%*	*68.1%*
AIR EXPANSION EFFICIENCY	*65.7%*	*77.6%*	*75.5%*	*31.9%*

As the pre-blowdown pressure ratio P_{C_1}/P_{B_1} increases from 1.0 to 1.3, the air expansion efficiency may drop by as much as 14 percentage points, all other operating parameters remaining equal. This point, together with the observations above, prescribes the operating strategy that leads to optimum performance of the hybrid internal combustion engine in air driving mode. At the beginning of an air driving event the pressure ratio above is 1.0. This ratio must be maintained at that value to minimize the loss in process 1-2. Consequently, we suggest that valve #2 remain open throughout an air driving event. When the pressure in the tank drops to a level near 4 atm, valve #2 is closed, the engine continues to get power from the compressed air in the EM, and fuel injection commences when the available energy in the manifold is not

enough to fulfill the energy demand of the vehicle. However, in our attempt to avoid modeling complexities, we are again limited to working with connections of 2 tanks at a time, and the strategy above calls for times in which merging of the contents of 3 tanks takes place. Therefore, the closest to the scheme above is to connect the tank and EM once at the beginning of every air driving engine cycle. In that case, the maximum pre-blowdown pressure ratio is 1.27, as given by Eq.(4.15).

Table 4-6. Relative Loss of Available Energy in Various Air Driving Events

Pre -Blowdown Conditions $P_{C_1} = 8\ atm$, $\frac{P_{C_1}}{P_{B_1}} = 1.33$	$\frac{P_{B_2}}{P_{A_2}} = 7.94$	$\frac{P_{B_2}}{P_{A_2}} = 7.94$	$\frac{P_{B_2}}{P_{A_2}} = 7.94$	$\frac{P_{B_2}}{P_{A_2}} = 7.94$
$W_{3\text{-}5}$ *(J/cyl-cycle)*	*52.3*	*106*	*180*	*13.9*
"IVC" (deg. ATC)	*24*	*40*	*63*	*0*
Pressure P_{A_5} *(atm)*	*0.55*	*1.0*	*2.0*	*0.31*
IRREVERSIBLE PROCESS	***RELATIVE LOSS OF AVAILABLE ENERGY***			
1-2	*48.1%*	*31.2%*	*19.0%*	*72.6%*
2-3	*15.1%*	*9.8%*	*6.1%*	*23.2%*
3'-4	*0.82%*	*0.61%*	*0.44%*	*0.00%*
5-6	*6.7%*	*0.00%*	*8.4%*	*20.9%*
6-7	*-25.1%*	*-16.2%*	*-9.9%*	*-38.0%*
7-8	*1.7%*	*5.9%*	*4.5%*	*0.03%*
TOTAL RELATIVE LOSS	*47.3%*	*31.4%*	*28.5%*	*78.7%*
AIR EXPANSION EFFICIENCY	*52.7%*	*68.6%*	*71.5%*	*21.3%*

The "intake valve" closing timing is chosen in a way that the power requirement in the CVS cycle is fulfilled while in-cylinder thermodynamic losses are minimized. When the tank pressure is kept above 4 atm, producing the average amount of driving work (52 J/cylinder-cycle) is always an achievable task. Hence, "IVC" timing must aimed at minimizing the loss in process 5-6. We recommend that valve #1 be closed at a point in the expansion stroke such that the cylinder pressure when the piston reaches BC is atmospheric, or very close to it on the high side. A vacuum inside the cylinder must be avoided. As the values in Tables 4-3 through 4-6 show, operation of the air motor in this manner results in net amounts of driving work that are

higher than the 52 J/cylinder-cycle average figure. In that case, cylinder disabling is used to control the amount of work transferred to the transmission input.

The losses resulting from blowdown process 2-3 and mixing process 3'-4 are not controllable. Since the cylinder pressure at state 2 is always atmospheric, the outcome of the unrestrained expansion of the air in the EM into the clearance volume of the cylinder depends strictly on the pressure of the EM at state 2, which in turn depends upon the initial tank pressure. When compared to the dissipation involved in other steps, the loss associated with process 3'-4 is insignificant. It is directly related to how late "IVC" occurs in the expansion stroke. Process 6-7, on the other hand, does not result in destruction of available energy. When the air in the tank absorbs heat from the wall, it gains available energy. In our calculation, when no blowdown occurs between the tank and the exhaust manifold, step 6-7 does not increase the available energy of the system.

If the recommended air driving strategy is used, that is, if the air pressure in the tank is not allowed to drop below 4 atm, and "IVC" timing is chosen so that the cylinder pressure at the end of the expansion stroke is atmospheric or slightly larger (never smaller), the smallest air expansion efficiency predicted by our model is 68.6%. So, the 65% value introduced in Chapter 2 for the air expansion efficiency seems suitable for most air driving events, particularly if blowdown process 1-2 between the tank and "IM" is minimized as suggested by our operating strategy. Fully variable valve timing and cylinder disabling are features required to minimize irreversibilities in operation and to control the work produced by the hybrid internal combustion engine in air motor mode.

Chapter 5 - Emissions

5.1 Problem Statement

As with any motor vehicle, engine-out and tailpipe emissions are a major concern in the operation of the hybrid internal combustion engine. The facts that the engine stops and then commences firing frequently, that it operates as an air compressor and air motor, and that cylinder disabling is used introduce new variables in the operation of the system. The new unknowns result in additional uncertainty in assessing the emissions performance of the hybrid engine. Engine-out emissions must be controlled, but the minimization of tailpipe emissions to the atmosphere is our main focus.

In an attempt to keep pollution at a minimum level, excessive cooling of the catalytic converter must be avoided. If pressurized air is inducted through the IM and expelled via the EM when the engine is operating as an air motor, the catalyst would cool down[2]. That is one reason why we chose to utilize the EM as the intake side of the engine and the IM as the exhaust side when in air motor mode, since this operating scheme reduces the original problem to that of having stationary exhaust gas in the converter. In the following sections, we propose a method to estimate the effects of operating the hybrid system and disabling cylinders on the performance of the catalytic converter.

5.2 Proposed Analysis

The CVS cycle represents 1373 seconds of typical urban driving. Our analysis of the hybrid internal combustion engine concept has thus far been based on the performance and power requirements of Ford's P2000 vehicle as it is driven throughout the cycle. A typical piece of the cycle can be divided in segments in which normal engine operation, air storage, and air driving take place. Using this information, a lumped thermal capacity model of the catalytic converter would be used to estimate the catalyst's cool down/warm up times as the mode of operation of the engine changes. This result would give an idea of how long it takes before the efficiencies of the converter drop below desired levels.

---

[2] The 1.8-litre Zetec engine we have used for our analysis is a 16-valve engine. A potential way to solve this problem is to have 2 exhausts systems (taking advantage of the two exhaust valves per cylinder), one connected to the catalyst and the other one connected to the air storage system. This adds complexity to the system, but is worth considering.

Alternatively, we have an emissions map for Ford's 1.8-litre Zetec engine containing data of HC, CO, and NO_x emissions as a function of engine speed and torque. These figures could be used in a way similar to that in which the fuel flow values were used in the available energy analysis simulation done for the hybrid internal combustion engine. After concluding this procedure, we would have estimates of total emissions of the hybrid vehicle in the CVS cycle.

5.3 Effect of Cylinder Disabling

The main purpose behind using cylinder disabling is to fire fewer cylinders in the engine at a higher load than all cylinders would operate at if all were firing. This results not only in more efficient performance, but also in higher burnt gas operating temperatures. Consequently, due to the higher gas temperatures, one would expect higher engine-out specific NO_x emissions, and probably lower engine-out specific HC emissions. Furthermore, the catalyst would be likely to exhibit a faster warm up time. The higher NO_x emissions can be reduced by retaining some exhaust gas inside the cylinders by the end of the exhaust stroke, a special type of EGR that is attainable by varying engine valve overlap when fully variable valve timing is an option. However, it should be pointed out that the use of any kind of EGR reduces the space in the cylinder that air and fuel may occupy, deviating performance from minimum bsfc level.

Chapter 6 - Summary of Results, Conclusions and Recommendations

6.1 Summary of Results

The basis of our available energy analysis of the hybrid internal combustion engine is the power requirement of the Ford Motor Company P2000 vehicle as it is driven through the CVS cycle (Federal Urban Driving Schedule). This was combined with fuel consumption data for the company's 1.8-litre Zetec engine and with estimates of engine friction to determine fuel consumption and economy for the vehicle with the pneumatic hybrid engine. The available energy analysis was done for conditions ranging from ideal to fully irreversible (no air storage/use capability) and for several operating conditions of the engine. The graph in Fig. 6-1 shows fuel consumption of the hybrid engine as a function of its air processing efficiency for the different schemes of operation of the system. The vehicle with the baseline engine consumes 651.3 g of fuel in the CVS cycle. Adding features like no use of fuel during braking and idle shut off, but no air storage/use (zero efficiency case), results in the engine's burning of 599.6 g and 549.3 g of fuel, respectively. This tells us that in the CVS cycle, leaving the engine on during braking costs 51.7 g of fuel (7.9% of baseline consumption), and idling the engine consumes another 50.3 g (7.7% of the total). Engine friction accounts for 93.8 g of fuel used (14% of the total).

When hybrid operation is fully ideal, the best attainable performance corresponds to a fuel consumption of 475.6 g of fuel, when the engine is never powered at idle. This represents a reduction of 175.7 g of fuel or 27% from the baseline. As the results below show, the introduction of cylinder disabling into engine operation has a significant effect in the reduction of fuel consumption. The baseline vehicle with cylinder disabling consumes 577.6 g of fuel, 11% less than the baseline, for a savings of 73.7 g. Under this condition, the minimum fuel consumption achievable with pneumatic hybridization is of 405.9 g of fuel, which represents a reduction of 38% from the unmodified Zetec engine. These results account for friction in the disabled cylinders. If engine friction is omitted, fuel usage comes down to a mere 190.7 g. This figure shows the significant role that engine friction has in reducing the benefit obtained from this hybrid concept.

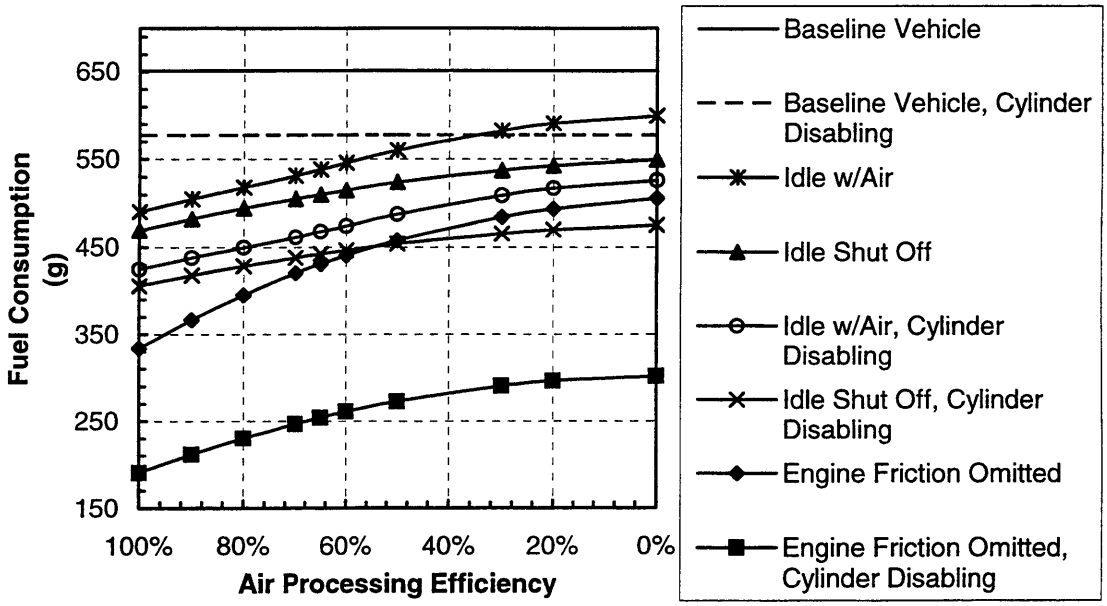

Figure 6-1. Fuel Consumed by the Hybrid Internal Combustion Engine in the CVS cycle vs. Air Processing Efficiency for Several Operating Conditions

Fuel consumption numbers give the most useful information about the performance of the hybrid internal combustion engine because they give the fuel savings directly. However, steady-state fuel economy values (in mpg) for the hybrid are easily comparable to those corresponding to current vehicles with conventional internal combustion engines. The flowchart in Fig. 6-2 shows how fuel economy for the P2000 vehicle evolves as different features of the concept are introduced into engine operation. One can see how the economy of 32.6 mpg for the baseline vehicle is incremented in several steps until it reaches 52.4 mpg when all the options of the hybrid engine are exploited and the system operates reversibly. Examining the values in the figure closely shows that, on average, pneumatic hybridization accounts for an improvement of at most 20% in steady-state fuel economy. The steady state fuel economy values corresponding to the ideal hybrid ($\eta_{a,p}$ = 100%) are about 20% higher than those for the 0% air processing efficiency case for the 4 possible configurations of the hybrid engine that account for engine friction.

The exact benefit obtained from the air storage and usage capability of the hybrid internal combustion engine depends on how efficient the air flow processes are. For that reason, we used simple models of braking and air driving events to obtain estimates for the air processing efficiency. For the braking case, the best performance is achieved when there is no blowdown process between the cylinder and the exhaust manifold (EM), the initial EM pressure

is kept above 4 atm, and the pre-blowdown pressure ratio between the EM and the storage tank is maintained below 1.1. The amount of braking work done exceeds the average requirement of the CVS cycle, so braking torque is controlled by disabling cylinders when appropriate. This results in a maximum air compression efficiency of $\eta_{a,c} \approx 85\%$. For less favorable operating conditions, this efficiency may reach negative values, meaning that an attempt to store available energy in the system fails, and some of the previously stored compressed air available energy is lost in the process. In an air driving event, best performance is accomplished when blowdown processes are minimized and the cylinder pressure when the piston reaches BC is 1 atm. Tank pressure is not allowed to drop below 4 atm. For this scenario, driving work also exceeds the average demand of the CVS cycle. Like in a braking event, cylinders are disabled as necessary to control driving work. The maximum air expansion efficiency estimated under these conditions is $\eta_{a,e} \approx 88\%$. This efficiency may also become negative when operation deviates from the scheme suggested in Chapter 4.

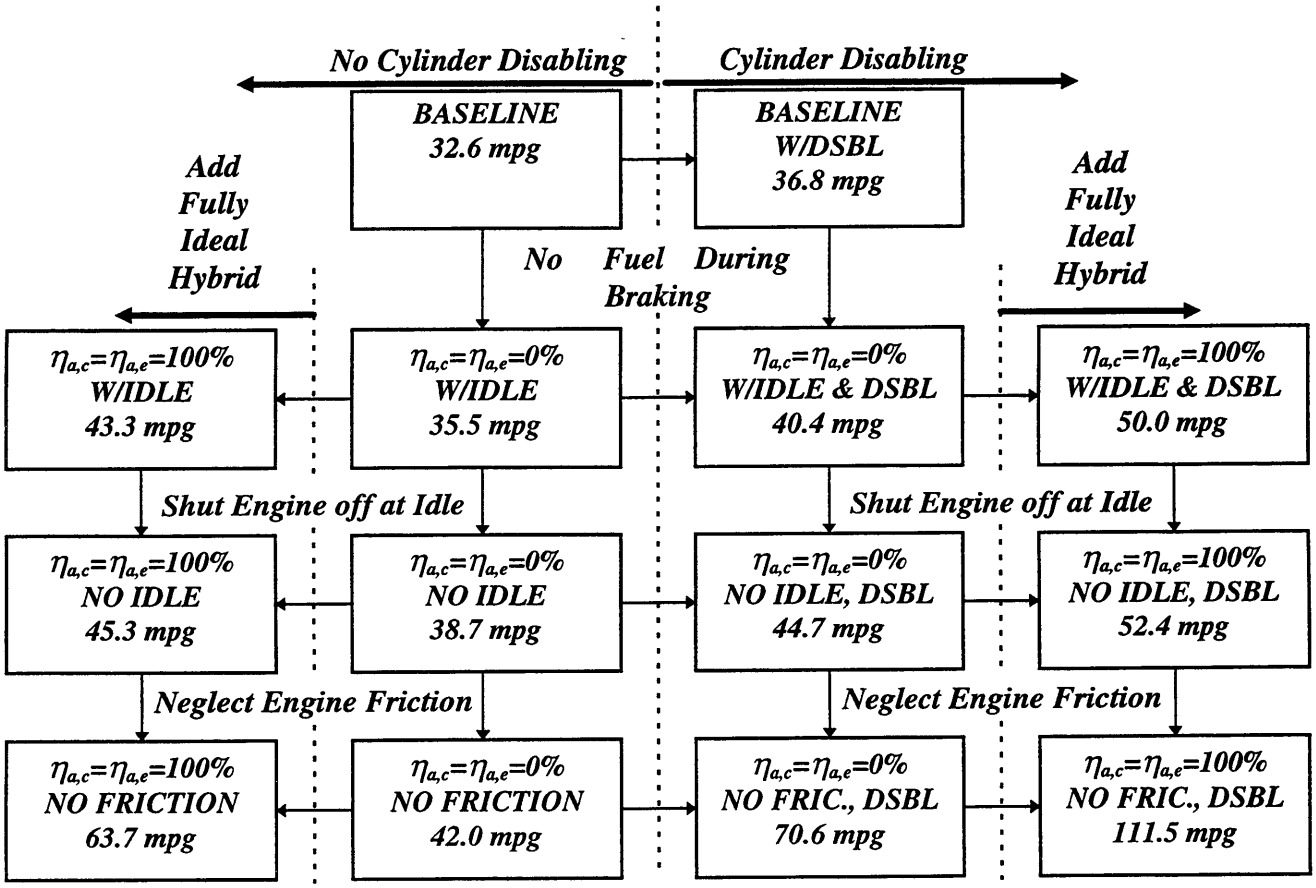

Figure 6-2. Individual Contributions to Hybrid Internal Combustion Engine Fuel Economy

In Chapter 2, we predicted that 65% was an appropriate value for the air processing efficiency, since it is a typical value for mechanical compressors and turbines. After carrying out an analysis of the irreversible processes involved in braking and air driving events in Chapter 4, we concluded that this is a suitable value to assume for this efficiency, since our models of the air storage and use processes are much simpler than those of the real processes, and initial temperatures in the manifold and tank, which were set arbitrarily, can reduce the air compression and expansion efficiencies. Table 6-1 shows fuel consumption and economy values for the different operating conditions of the hybrid engine at an air processing efficiency of 65%. In its optimum mode of operation at this efficiency, when air storage and use capabilities are utilized, the engine is shut off at idle, and cylinder disabling is used (including the effect of friction in the non firing cylinders in our model), the hybrid internal combustion engine consumes 32% less fuel than the baseline Zetec engine, yielding 48.1 mpg.

Table 6-1. Results of Available Energy Analysis for $\eta_{a,p} = 65\%$ vs. Mode of Operation of Hybrid Internal Combustion Engine

Mode of Operation	Mass of Fuel Used (g)	Fuel Economy (mpg)	Reduction in Fuel Consumption Relative to Baseline (%)	Reduction in Fuel Consumption Relative to Baseline w/Disabling (%)
Baseline, 1.8-litre Zetec Engine	***651.3***	***32.6***		
Hybrid, Idle the Engine	*538.6*	*39.5*	*17*	
Hybrid, Do not Idle	*510.3*	*41.7*	*22*	
Hybrid, No Engine Friction	*430.7*	*49.4*	*34*	
Baseline, 1.8-litre Zetec Engine w/Cyl. Disabling	***577.6***	***36.8***	***11***	
Hybrid w/Disabling, Idle the Engine	*468.0*	*45.4*	*28*	*19*
Hybrid w/Disabling, Do not Idle	*442.5*	*48.1*	*32*	*23*
Hybrid w/Disabling, No Engine Friction	*254.1*	*83.7*	*61*	*56*

6.2 Remarks and Future Work

As the results from our available energy analysis of the hybrid internal combustion engine show, engine friction reduces the benefit of this concept substantially. Similarly, minimization of the thermodynamic irreversibilities involved in the air storage and use processes is essential for satisfactory performance of the hybrid part of the system. This requires fully variable valve timing and cylinder disabling (when operating with air). However, introducing fully variable valve timing modifications to the operating scheme of a conventional engine with no air storage/use capabilities yields considerable improvements in fuel economy. The benefit results from not injecting fuel into the engine during braking events, from idle shut off, and most importantly, from the use of cylinder disabling during firing to minimize throttling losses. Ultimately, the air processing efficiency, as well as the costs associated with implementing the necessary changes on the conventional engine, determine what the additional improvement in fuel consumption is as a result of hybrid operation.

After examining the results of our analysis, several issues that deserve further research come to mind, all of which are aimed at improving the performance of the conventional internal combustion engine. As discussed above, engine friction has a major effect in reducing the benefit of pneumatic hybridization and cylinder disabling. Therefore, possible means to reduce its magnitude is a topic of great interest. Fully variable valve timing modifications, as well as cylinder disabling have a favorable effect on fuel economy. However, their effects on engine-out emissions is not quantified. Models could be developed to determine how the implementation of both strategies affects the emissions performance of the engine. Furthermore, the effect of cylinder disabling on engine friction must be explored, since it is claimed that, if a certain disabling scheme is followed, it may effectively reduce dissipation.

The issue of engine restarting is not explored in our model. Whenever the engine is shut off at idle, we assume that the energy required to bring it up to the required speed is that necessary to overcome engine friction and fulfill the requirements of the CVS cycle. Accelerating the engine from rest to an idling speed of 880 rpm requires 823.75 J of energy, approximately 73% of the 1126.79 J required to overcome engine friction during a second of idling. If we choose to shut the engine off at idle, there are 17 starts in the CVS cycle. The engine, though, is supposed to idle for 262 seconds. Hence, the startup energy is negligible when compared to the energy savings resulting from idle shut off.

The tank volume assumed for our analysis is 80 liters. Since we are carrying out an available energy analysis, our estimates of fuel economy are insensitive to tank size. The size of

the tank becomes an issue when considering thermodynamic losses. In particular, it becomes very important when packaging of all the components in the engine compartment of a vehicle is explored.

References

1. "Energy Distribution in a Mid-Size Vehicle". Flowchart prepared at Ford Motor Co.

2. Moyer, D.F., Patents on Hybrid Internal Combustion Engine.

3. Heywood, J.B., "Internal Combustion Engine Fundamentals", McGraw-Hill, New York, 1988.

4. Patton, K.J., Nitschke, R.G., and Heywood, J.B., "Development and Evaluation of a Friction Model for Spark-Ignition Engines", SAE Paper 890836, 1989.

5. Nunney, M.J., "The Automotive Engine", Newnes-Butterworths, London, 1975.

6. Huang, F.F., "Engineering Thermodynamics", Macmillan Publishing Co., New York, 1976.

7. "Bosch Automotive Handbook" (3rd Ed.), Robert Bosch GmbH, Stuttgart, 1993.

8. Gillespie, T.D., "Fundamentals of Vehicle Dynamics", SAE, Warrendale, 1992.

9. "Automotive Electric/Electronic Systems" (1st Ed.), Robert Bosch GmbH, Stuttgart, 1988.

10. Amann, C.A., "Air-Injection Supercharging – A Page from History", SAE Paper 920843, 1992.

11. Kociba, R. and Parr, M.D., "The General Motors Supercharged 3800 Engine", SAE Paper 910685, 1991.

12. Hitomi, M., Yusuriha, Y., and Tanaka, K., "The Characteristics of Pressure Wave Supercharged Small Diesel Engine", SAE Paper 890454, 1989.

13. Alsterfalk, M., Filipi, Z.S., and Assanis, D.N., "The Potential of the Variable Stroke Spark-Ignition Engine", SAE Paper 970067, 1997.

14. Kim, D.H., Anderson, M.D., Tsao, T., and Levin, M., "Dynamic Model of a Springless Electrohydraulic Valvetrain", SAE Paper 970248, 1997.

15. Henry, R., Lequesne, B., "A Novel, Fully Flexible, Electro-Mechanical Engine Valve Actuation System", SAE Paper 970249, 1997.

16. Meistrick, Z., "Jacobs New Engine Brake Technology", SAE Paper 922448, 1992.

17. Göhring, E., von Glasner, E., and Povel, R., "Engine Braking Systems and Retarders - An Overview from an European Standpoint", SAE Paper 922451, 1992.

18. Newton, K., Steeds, W., Garrett, T., "The Motor Vehicle" (11th Ed.), Butterworths, London, 1989.

19. Moriya, Y., Watanabe, A., Uda, H., Kawamura, H., Yoshioka, M., and Adachi, M., "A Newly Developed Intelligent Variable Valve Timing System - Continuously Controlled Cam Phasing as Applied to a New 3 Liter Inline 6 Engine", SAE Paper 960579, 1996.

20. Duckworth, R. and Barker, L., "A Comparative Study of Variable Camshaft Phasing and Part Throttling for Performance and Emissions", SAE Paper 960580, 1996.

21. Li, P., Adamczyk, A., and Pakko, J., "Thermal Management of Automotive Emission Systems: Reducing the Environmental Impact", The Japan-U.S. Seminar on Thermal Engineering for Global Environment Protection.

22. Heck, R., and Farrauto, R., "Catalytic Air Pollution Control", Van Nostrand Reinhold, New York, 1995.

Appendix A - Analysis of Reversible Adiabatic Available Energy Storage/Withdrawal

For a reversible adiabatic process involving the control volume (dashed line) in Fig. 2-1, the first law of thermodynamics is

$$\frac{dE_{cv}}{dt} = -\dot{W} + \sum(\dot{m}h)_{in} - \sum(\dot{m}h)_{out} . \tag{A.1}$$

The second law states that

$$\frac{dS_{cv}}{dt} = \sum(\dot{m}s)_{in} - \sum(\dot{m}s)_{out} , \tag{A.2}$$

and the ideal gas law gives

$$PV_T = m_{cv}RT . \tag{A.3}$$

In general, $E_{cv} = m_{cv}c_v T$, which implies that

$$\frac{dE_{cv}}{dt} = c_v\left(T\frac{dm_{cv}}{dt} + m_{cv}\frac{dT}{dt}\right). \tag{A.4}$$

Differentiating Eq.(A.3), we get

$$\frac{V_T}{R}\frac{dP}{dt} = \left(T\frac{dm_{cv}}{dt} + m_{cv}\frac{dT}{dt}\right). \tag{A.5}$$

Substituting Eq.(A.5) into Eq.(A.4), we finally have

$$\frac{dE_{cv}}{dt} = \frac{c_v}{R}V_T\frac{dP}{dt} . \tag{A.6}$$

The entropy inside the control volume, S_{cv}, is equivalent to $m_{cv}s_{cv}$, where s_{cv} represents the specific entropy inside the system. Entropy relative to atmospheric conditions is defined as

$$S_{cv} = m_{cv}s_{cv} = m_{cv}\left(c_p \ln\frac{T}{T_a} - R\ln\frac{P}{P_a}\right). \tag{A.7}$$

Storing Air

The air storage mode is of relevance in a braking event satisfying $W_{\tan k} = \dot{W}_{net} \cdot 1\ \text{sec} < 0$. In this situation, mass conservation has

$$\frac{dm_{cv}}{dt} = \dot{m} . \tag{A.8}$$

The specific enthalpy flow out of the control volume is zero, and the flow into it is given by

$$h_{in} = c_p T_a . \tag{A.9}$$

By the same reasoning, the specific entropy leaving is also zero, and that coming in is equivalent to

$$s_{in} = c_p \ln\frac{T_a}{T_a} - R\ln\frac{P_a}{P_a} = 0 . \tag{A.10}$$

If we substitute Eqs. (A.3), (A.6), (A.8), and (A.9) into Eq.(A.1) and write the latter in differential form, we obtain $\frac{c_v}{R} V_T dP = -dW + c_p T_a dm_{cv}$. Integrating this result yields

$$\frac{c_v}{R} V_T \left(P_f - P_i\right) = -W_{tank} + c_p T_a \left(m_{cv_f} - m_{cv_i}\right) = -W_{tank} + \frac{c_p}{R} V_T T_a \left(\frac{P_f}{T_f} - \frac{P_i}{T_i}\right). \tag{A.11}$$

Solving for P_f, the pressure inside the tank at the end of the second of the CVS cycle in question, we get

$$P_f = \frac{P_i V_T \left[\frac{T_a}{T_i}\left(\frac{c_v}{R}+1\right) - \frac{c_v}{R}\right] + W_{tank}}{V_T \left[\frac{T_a}{T_f}\left(\frac{c_v}{R}+1\right) - \frac{c_v}{R}\right]} . \tag{A.12}$$

Inserting the results of Eqs. (A.3), (A.7), (A.8), and (A.10) into the second law of thermodynamics, Eq.(A.2), and integrating, we have

$$dS_{cv} = 0 \Rightarrow S_{cv_f} - S_{cv_i} = \frac{V_T}{R}\left[\frac{P_f}{T_f}\left(c_p \ln\frac{T_f}{T_a} - R\ln\frac{P_f}{P_a}\right) - \frac{P_i}{T_i}\left(c_p \ln\frac{T_i}{T_a} - R\ln\frac{P_i}{P_a}\right)\right] = 0 . \tag{A.13}$$

Solving the system of equations consisting of Eqs. (A.12) and (A.13) for the pressure and temperature of the contents of the tank at the end of each second completely defines the final state, since the mass of can be computed via Eq.(A.3).

Consuming Air

Modeling the processes that occur when air is being extracted from the tank is a more complex task than dealing with air storage processes. Air has to be withdrawn from the tank either to accelerate the vehicle or to overcome engine friction through a given second of the CVS cycle. Whenever work is delivered from the tank, $W_{tank} > 0$, and air is consumed.

In this case, mass conservation has that

$$\frac{dm_{cv}}{dt} = -\dot{m}. \tag{A.14}$$

The specific enthalpy flow is governed by

$$h_{in} = 0,\ h_{out} = c_p T. \tag{A.15}$$

The specific entropy flow through the system's boundary is given by

$$s_{in} = 0,\ s_{out} = c_p \ln\frac{T}{T_a} - R\ln\frac{P_a}{P_a} = c_p \ln\frac{T}{T_a}. \tag{A.16}$$

Substituting Eqs. (A.3), (A.6), (A.14), and (A.15) into Eq.(A.1), we obtain

$$\frac{c_v}{R}V_T\frac{dP}{dt} = -\frac{dW_{tank}}{dt} + c_p T\frac{dm_{cv}}{dt} = -\dot{W}_{tank} + \frac{c_p}{R}V_T P\frac{\dot{m}_{cv}}{m_{cv}}. \tag{A.17}$$

The time derivative of the entropy inside the control volume is given, from Eq.(A.7), to be

$$\frac{dS_{cv}}{dt} = m_{cv}\left(c_p\frac{\dot{T}}{T} - R\frac{\dot{P}}{P}\right) + \dot{m}_{cv}\left(c_p\ln\frac{T}{T_a} - R\ln\frac{P}{P_a}\right). \tag{A.18}$$

From Eq.(A.3), the ideal gas law, we find that

$$\dot{T} = \frac{V_T}{R}\left(\frac{\dot{P}}{m_{cv}} - P\frac{\dot{m}_{cv}}{m_{cv}^2}\right) \Rightarrow \frac{\dot{T}}{T} = \frac{\dot{P}}{P} - \frac{\dot{m}_{cv}}{m_{cv}}, \tag{A.19}$$

which when plugged into Eq.(A.18) yields

$$\frac{dS_{cv}}{dt} = m_{cv}c_v\frac{\dot{P}}{P} - c_p\dot{m}_{cv} + \dot{m}_{cv}\left(c_p\ln\frac{T}{T_a} - R\ln\frac{P}{P_a}\right). \tag{A.20}$$

Inserting Eqs. (A.14), (A.16), and (A.20) into Eq.(A.2), we finally get

$$c_v m_{cv}\frac{\dot{P}}{P} - c_p\dot{m}_{cv} - R\dot{m}_{cv}\ln\frac{P}{P_a} = 0. \tag{A.21}$$

The state of the air at the end of each second of interest may be obtained by solving the differential equations (A.17) and (A.21) numerically for P_f and m_{cv_f}, and computing the final temperature using Eq.(A.3).

Appendix B - Analysis of Reversible Isothermal Available Energy Storage/Withdrawal

For a reversible isothermal process involving the system shown Fig. 2-1, the first law of thermodynamics is

$$\frac{dE_{cv}}{dt} = \dot{Q} - \dot{W} + \sum(\dot{m}h)_{in} - \sum(\dot{m}h)_{out} . \tag{B.1}$$

The second law states that

$$\frac{dS_{cv}}{dt} = \frac{\dot{Q}}{T_a} + \sum(\dot{m}s)_{in} - \sum(\dot{m}s)_{out} , \tag{B.2}$$

and the ideal gas law gives

$$PV_T = m_{cv} RT_a . \tag{B.3}$$

The case explored in this analysis is that when the air inside the tank is initially at atmospheric temperature and remains at it throughout the whole set of processes involved in braking and accelerating the vehicle. Hence, the air that crosses the boundary of the control volume when air is being stored is at the same state as that which is removed when powering the vehicle. Consequently, it follows that the specific expressions of the first and second laws of thermodynamics that apply to the air storage mode are mathematically identical to those pertinent to the air consumption mode. For simplicity, let us work out the equations corresponding to the air storage case.

Equations (A.6), (A.8), (A.9), and (A.10) remain valid for this scenario. After substituting them into Eq.(B.1), we get, in differential form,

$$\frac{c_v}{R} V_T dP = dQ_{TOT} - dW_{del} + c_p T_a dm_{cv} . \tag{B.4}$$

Inserting Eq.(B.3) into Eq.(B.4) and integrating, we obtain

$$\frac{c_v}{R} V_T \left(P_f - P_i\right) = Q_{TOT} - W_{tank} + c_p T_a \frac{V_T}{RT_a}\left(P_f - P_i\right) \Rightarrow W_{tank} - Q_{TOT} = \left(P_f - P_i\right) V_T . \tag{B.5}$$

Substituting Eq.(A.10) into Eq.(B.2) and writing the result in differential form, we get for the second law of thermodynamics

$$dS_{cv} = \frac{1}{T_a} dQ_{TOT} \Rightarrow S_{cv_f} - S_{cv_i} = m_{cv_f} s_{cv_f} - m_{cv_i} s_{cv_i} = \frac{Q_{TOT}}{T_a} . \tag{B.6}$$

Using Eqs. (A.7) and (B.3), we rewrite Eq.(B.6) as

$$V_T\left(P_i \ln\frac{P_i}{P_a} - P_f \ln\frac{P_f}{P_a}\right) = Q_{TOT}\,. \tag{B.7}$$

Inserting Eq.(B.7) into Eq.(B.5) finally yields the result given above as Eq.(2.13),

$$V_T\left(P_i \ln\frac{P_i}{P_a} - P_f \ln\frac{P_f}{P_a}\right) - W_{tank} = \left(P_i - P_f\right)V_T\,, \tag{B.8}$$

which may be solved for P_f, the final tank pressure that when plugged into Eq.(B.7) gives the net heat transfer into the system.

Appendix C - Output of Available Energy Analysis Simulation

For Air:

R	287 J/kg K
c_v	719 J/kg K
c_p	1006 J/kg K
γ	1 40
P_{atm}	1.013E+05 Pa
T_{atm}	300 K

Ford Motor Co. 1.8 L Zetec Engine

Bore	80 6 mm
Stroke	88.0 mm
Total Disp.	1795 98 cm^3
Air Tank Volume	0 08 m^3
Total Distance Driven	11.920 km / 7.450 miles

Q_{LHV}	44.83 MJ/kg
η_{fu}	35%
Fuel Density	0.754 kg/L
Quadratic Polynomial Fit for Fuel Flow near Zero Torque	3 455E-11 / 2.454E-08 / 1 436E-04
Consumption and Fuel Economy of Conventional Engine	0.228 gal / 651.3 g / 32.6 mpg
Consumption and Fuel Economy of Conventional Engine w/Cyl. Disabling	0.202 gal / 577.6 g / 36.8 mpg

RATIOS OF INTEREST

Work Stored to Work Ava. at Trans.	64.85%
Actual Work Withdrawn to Work Req'd. at Trans.	23.88%
Work Req'd at Trans. to Desired Withdrawn Work	59.18%

Engine Friction Neglected	NO
tfmep adjusted by	0 75
$\eta_{a,e}$	100%
$\eta_{a,e}$	100%

	w/o Disabling	w/Disabling	
Actual Fuel Savings:	0.064	0.086	gallons
	181.8	245.5	grams
	45.3	52.4	mpg
	27.91%	37.69%	of max
Comparison w/baseline	139%	142%	

Time (s)	Speed (km/h)	Accel. (m/s^2)	Eng. Speed (rpm)	Power at Trans. Input (W)	Total Friction Mean Effective Press. tfmep (Pa)	Power Dissipated Due to Engine Friction (W)	Net Power that must be Transferred from the Air Inside the Tank (W)	Engine's Power Conversion ("Mechanical") Eff.	Initial Tank Pressure (Pa)	Initial Tank Temp. (K)	Initial Tank Mass (kg)	Tank's Initial Ava. Energy (J)	Tank's Final Ava. Energy (J)	Change in Tank's Ava. Energy (J)	Final Tank Pressure (Pa)	Final Tank Temp. (K)	Final Tank Mass (kg)
0	0 00	0.00	880.00	0.00	8.555E+04	1126.79	0 00	N/A	4.03E+05	300	0.374	20,348.77	20,348 77	0.00	4.03E+05	300	0.374
1	0.00	0.00	880 00	0.00	8.555E+04	1126.79	0.00	N/A	4.03E+05	300	0.374	20,348.77	20,348.77	0.00	4.03E+05	300	0.374
2	0.00	0.00	880.00	0.00	8.555E+04	1126.79	0 00	N/A	4 03E+05	300	0.374	20,348 77	20,348.77	0.00	4.03E+05	300	0.374
3	0.00	0.00	880.00	0.00	8.555E+04	1126.79	0 00	N/A	4 03E+05	300	0.374	20,348.77	20,348.77	0.00	4.03E+05	300	0.374
4	0.00	0 00	880.00	0.00	8.555E+04	1126.79	0.00	N/A	4.03E+05	300	0.374	20,348.77	20,348.77	0.00	4.03E+05	300	0.374
5	0.00	0.00	880.00	0.00	8.555E+04	1126.79	0 00	N/A	4.03E+05	300	0.374	20,348.77	20,348.77	0.00	4.03E+05	300	0.374
6	0.00	0.00	880.00	0.00	8.555E+04	1126.79	0.00	N/A	4.03E+05	300	0.374	20,348.77	20,348.77	0.00	4.03E+05	300	0.374
7	0.00	0.00	880.00	0.00	8.555E+04	1126.79	0.00	N/A	4 03E+05	300	0.374	20,348.77	20,348.77	0.00	4.03E+05	300	0 374
8	0.00	0.00	880 00	0.00	8.555E+04	1126.79	0.00	N/A	4 03E+05	300	0.374	20,348.77	20,348.77	0.00	4.03E+05	300	0.374
9	0.00	0.00	880.00	0.00	8.555E+04	1126.79	0.00	N/A	4 03E+05	300	0.374	20,348.77	20,348.77	0.00	4.03E+05	300	0.374
10	0.00	0.00	880.00	0.00	8.555E+04	1126.79	0.00	N/A	4.03E+05	300	0.374	20,348.77	20,348.77	0.00	4.03E+05	300	0.374
11	0.00	0.00	880.00	0.00	8.555E+04	1126 79	0.00	N/A	4.03E+05	300	0.374	20,348.77	20,348.77	0.00	4.03E+05	300	0.374
12	0.00	0.00	880.00	0.00	8.555E+04	1126.79	0.00	N/A	4 03E+05	300	0.374	20,348.77	20,348.77	0.00	4.03E+05	300	0.374
13	0.00	0 00	880.00	0.00	8.555E+04	1126.79	0.00	N/A	4 03E+05	300	0.374	20,348.77	20,348.77	0.00	4.03E+05	300	0.374
14	0.00	0.00	880.00	0.00	8.555E+04	1126.79	0.00	N/A	4.03E+05	300	0.374	20,348.77	20,348.77	0.00	4.03E+05	300	0.374
15	0.00	0.00	880.00	0.00	8.555E+04	1126.79	0 00	N/A	4.03E+05	300	0.374	20,348.77	20,348.77	0.00	4.03E+05	300	0.374
16	0.00	0.00	880.00	0.00	8.555E+04	1126.79	0.00	N/A	4.03E+05	300	0.374	20,348.77	20,348.77	0.00	4.03E+05	300	0.374
17	0.00	0.00	880.00	0.00	8.555E+04	1126.79	0.00	N/A	4.03E+05	300	0.374	20,348.77	20,348 77	0.00	4.03E+05	300	0.374
18	0.00	0.00	880.00	0.00	8.555E+04	1126.79	0.00	N/A	4.03E+05	300	0.374	20,348.77	20,348.77	0.00	4.03E+05	300	0.374
19	0.00	0.00	880.00	0.00	8.555E+04	1126.79	0.00	N/A	4.03E+05	300	0.374	20,348.77	20,348.77	0.00	4.03E+05	300	0.374
20	0.00	0.00	880.00	0.00	8.555E+04	1126 79	0.00	N/A	4.03E+05	300	0.374	20,348.77	20,348.77	0.00	4.03E+05	300	0.374
21	4.80	1.33	880.00	2915.44	8.555E+04	1126.79	4042.23	72.12%	4.03E+05	300	0.374	20,348.77	16,306.54	-4,042.23	3.65E+05	300	0.339
22	9 44	1.29	1148.82	5543.28	9.062E+04	1558.16	7101.44	78.06%	3.65E+05	300	0.339	16,306.54	9,205 10	-7,101.44	2.89E+05	300	0.268
23	13.76	1.20	1674.55	7560.99	1.021E+05	2558.95	10119 94	74.71%	2.89E+05	300	0.268	9,205.10	0.00	-9,205.10	1.01E+05	300	0.094
24	18.40	1.29	2239.22	10865.68	1.167E+05	3912.49	14778.18	73.53%	1.01E+05	300	0.094	0.00	0.00	0.00	1.01E+05	300	0.094
25	22.88	1.24	2784 42	13130.68	1.331E+05	5548.72	18679.40	70.29%	1.01E+05	300	0.094	0.00	0.00	0.00	1.01E+05	300	0.094
26	27.04	1 16	2057.04	14410.63	1.118E+05	3440.71	17851.33	80.73%	1.01E+05	300	0.094	0 00	0.00	0.00	1.01E+05	300	0.094
27	27.68	0 18	2105.72	2588.22	1.131E+05	3563.36	6151.57	42.07%	1.01E+05	300	0.094	0.00	0.00	0.00	1.01E+05	300	0.094
28	28.96	0.36	2203.10	4599.26	1.157E+05	3816.14	8415.40	54.65%	1.01E+05	300	0.094	0.00	0.00	0.00	1.01E+05	300	0.094
29	33.12	1.16	2519.57	14964.25	1.249E+05	4709.91	19674.16	76 06%	1 01E+05	300	0.094	0.00	0.00	0.00	1.01E+05	300	0.094
30	34.72	0.44	2641.28	6796.93	1.286E+05	5084.69	11881 62	57.21%	1 01E+05	300	0.094	0.00	0.00	0.00	1.01E+05	300	0.094
31	35.84	0.31	1848.29	5245.74	1.064E+05	2942.02	8187.76	64.07%	1.01E+05	300	0.094	0.00	0.00	0.00	1.01E+05	300	0.094
32	36.00	0.04	1856.54	1778.42	1.066E+05	2960.92	4739.34	37.52%	1 01E+05	300	0 094	0.00	0.00	0.00	1.01E+05	300	0.094
33	35.36	-0.18	1823.54	-862.99	1.057E+05	2885.72	2022.73	0.00%	1 01E+05	300	0 094	0.00	0.00	0.00	1.01E+05	300	0.094
34	34.40	-0.27	1774.03	-1887.43	1.045E+05	2774.85	887.42	0.00%	1.01E+05	300	0 094	0.00	0.00	0.00	1.01E+05	300	0.094
35	33.44	-0.27	1724.52	-1859.95	1 033E+05	2666.27	806.32	0.00%	1 01E+05	300	0.094	0 00	0.00	0.00	1.01E+05	300	0.094
36	32.64	-0.22	1683.27	-1351.78	1.023E+05	2577.51	1225.73	0.00%	1.01E+05	300	0.094	0.00	0.00	0.00	1.01E+05	300	0.094
37	31.68	-0.27	1633.76	-1803.16	1.011E+05	2473.02	669.86	0.00%	1.01E+05	300	0.094	0 00	0.00	0.00	1.01E+05	300	0.094
38	27.20	-1.24	1402.72	-10135.52	9.591E+04	2013.51	-8122.01	80.13%	1.01E+05	300	0.094	0 00	8,122.01	8,122.01	2.76E+05	300	0.256
39	23.84	-0.93	1229 44	-6570.22	9.225E+04	1697 44	-4872.78	74.16%	2.76E+05	300	0.256	8,122.01	12,994.79	4,872.78	3.31E+05	300	0.308
40	23.84	0.00	1229.44	616.26	9.225E+04	1697 44	2313.70	26.64%	3.31E+05	300	0.308	12,994 79	10,681.09	-2,313.70	3.06E+05	300	0.284
41	24.32	0 13	1850.12	1749.93	1.064E+05	2946.19	4696.12	37.26%	3 06E+05	300	0.284	10,681 09	5,984.97	-4,696.12	2.47E+05	300	0.230
42	24.80	0 13	1886.63	1874.96	1.073E+05	3030.39	4905.34	38 22%	2.47E+05	300	0.230	5,984.97	1,079.63	-4,905.34	1.58E+05	300	0.147
43	25.60	0.22	1947.49	2766.83	1.089E+05	3173.60	5940.43	46.58%	1.58E+05	300	0 147	1,079.63	0.00	-1,079.62	1.01E+05	300	0.094
44	27 36	0.49	2081.38	5623.45	1.124E+05	3501.72	9125.17	61 63%	1.01E+05	300	0 094	0 00	0.00	0.00	1.01E+05	300	0.094
45	30.56	0.89	2324.82	10778.94	1 192E+05	4146.53	14925 46	72.22%	1 01E+05	300	0.094	0 00	0.00	0 00	1 01E+05	300	0.094
46	33.76	0 89	2568.25	11999.44	1.264E+05	4857.68	16857.12	71.18%	1.01E+05	300	0 094	0.00	0.00	0.00	1 01E+05	300	0.094
47	36.32	0.71	1873.05	10576.50	1.070E+05	2998.91	13575 41	77.91%	1.01E+05	300	0 094	0 00	0.00	0.00	1.01E+05	300	0.094
48	36.64	0 09	1889.55	2367.56	1.074E+05	3037 17	5404.73	43.81%	1 01E+05	300	0.094	0.00	0.00	0.00	1 01E+05	300	0 094
49	36.32	-0 09	1873.05	219.33	1.070E+05	2998.91	3218 24	6 82%	1 01E+05	300	0 094	0 00	0.00	0.00	1 01E+05	300	0 094
50	36.16	-0 04	1864 79	739.34	1.068E+05	2979.88	3719.22	19.88%	1 01E+05	300	0 094	0 00	0.00	0.00	1 01E+05	300	0.094
51	34 08	-0.58	1757 53	-5328.89	1.041E+05	2738.40	-2590.49	48.61%	1.01E+05	300	0 094	0 00	2,590.49	2,590.49	1 93E+05	300	0.179
52	30.40	-1.02	1567.75	-9123 76	9.960E+04	2337.09	-6786 67	74 38%	1 93E+05	300	0.179	2,590.49	9,377.16	6,786.67	2.91E+05	300	0.270
53	27.36	-0.84	1410.97	-6712.45	9.609E+04	2029.15	-4683.30	69 77%	2.91E+05	300	0.270	9,377.16	14,060.46	4,683.30	3.42E+05	300	0.318
54	25 28	-0.58	1303.71	-4090.27	9 379E+04	1830.03	-2260 24	55.26%	3 42E+05	300	0 318	14,060.46	16,320.70	2,260.24	3.65E+05	300	0.339
55	25 28	0.00	1303.71	676.54	9.379E+04	1830.03	2506.57	26 99%	3.65E+05	300	0.339	16,320.70	13,814 13	-2,506.57	3.40E+05	300	0.316
56	28.32	0.84	1460.48	8820.93	9.718E+04	2124 18	10945.11	80.59%	3.40E+05	300	0.316	13,814.13	2,869.02	-10,945.11	1.98E+05	300	0.184
57	31.68	0.93	2410.02	10951.46	1.216E+05	4387.64	15339.10	71 40%	1 98E+05	300	0.184	2,869.02	0.00	-2,869.02	1.01E+05	300	0.094
58	34 56	0 80	2629.11	11191.48	1.282E+05	5046.41	16237 89	68.92%	1.01E+05	300	0.094	0.00	0.00	0.00	1.01E+05	300	0.094
59	37.12	0.71	1914.30	10832.70	1.080E+05	3095.05	13927.76	77.78%	1.01E+05	300	0.094	0.00	0.00	0 00	1 01E+05	300	0.094
60	38.72	0.44	1996.82	7178.47	1.102E+05	3292.37	10470.84	68.56%	1 01E+05	300	0.094	0.00	0.00	0.00	1.01E+05	300	0.094
61	39.36	0.18	2029.82	3804.35	1.110E+05	3373.21	7177 56	53.00%	1 01E+05	300	0.094	0.00	0.00	0.00	1.01E+05	300	0.094
62	39.84	0 13	2054.57	3275 37	1.117E+05	3434.57	6709.94	48.81%	1 01E+05	300	0.094	0.00	0.00	0.00	1.01E+05	300	0.094
63	40.00	0 04	2062.83	2108.91	1.119E+05	3455.16	5564 07	37 90%	1.01E+05	300	0.094	0.00	0.00	0.00	1.01E+05	300	0.094
64	39 36	-0.18	2029.82	-825.04	1.110E+05	3373.21	2548 17	0.00%	1.01E+05	300	0.094	0.00	0.00	0 00	1 01E+05	300	0.094
65	39.20	-0.04	2021.57	901 12	1.108E+05	3352.90	4254 02	21.18%	1.01E+05	300	0 094	0.00	0.00	0.00	1.01E+05	300	0.094
66	39.52	0 09	2038.07	2649.83	1 113E+05	3393.59	6043.43	43.85%	1 01E+05	300	0.094	0.00	0.00	0.00	1.01E+05	300	0.094
67	39.68	0.04	2046.32	2080.85	1.115E+05	3414.05	5494.89	37 87%	1.01E+05	300	0.094	0.00	0.00	0.00	1.01E+05	300	0.094
68	39 52	-0.04	2038.07	919.07	1.113E+05	3393.59	4312.66	21.31%	1 01E+05	300	0.094	0.00	0.00	0 00	1.01E+05	300	0 094
69	39 36	-0.04	2029.82	910.07	1.110E+05	3373.21	4283.28	21.25%	1.01E+05	300	0.094	0.00	0.00	0.00	1.01E+05	300	0.094
70	39 36	0.00	2029.82	1481.55	1.110E+05	3373.21	4854.76	30.52%	1.01E+05	300	0.094	0.00	0.00	0 00	1.01E+05	300	0.094

Can the Energy Requirement of the Vehicle be met in full using air?	Total Heat Transfer (J)	Engine Brake Torque (Torque at the Transmission Input) (Nm)	Approximate Amount of Fuel Used in WHOLE Sec (Conventional Engine) (g)	MASS OF FUEL USED WITH HYBRID (Using 4 cylinders) (g)	VOLUME OF FUEL SAVED WITH HYBRID (Using 4 cylinders) (gal)	MASS OF FUEL USED IN CONVENTIONAL ENGINE (Disabling Cylinders) (g)	MASS OF FUEL USED WITH HYBRID (Disabling Cylinders) (g)	VOLUME OF FUEL SAVED WITH HYBRID (Disabling Cylinders) (gal)	Minimum Number of Cylinders that Must Be Used
NO IDLE	0.00	0.00	0.192	0.000	6.727E-05	0.192	0.000	6.727E-05	NO FIRE
NO IDLE	0.00	0.00	0.192	0.000	6.727E-05	0.192	0.000	6.727E-05	NO FIRE
NO IDLE	0.00	0.00	0 192	0.000	6 727E-05	0.192	0 000	6.727E-05	NO FIRE
NO IDLE	0.00	0.00	0 192	0.000	6.727E-05	0.192	0 000	6.727E-05	NO FIRE
NO IDLE	0.00	0.00	0.192	0.000	6.727E-05	0.192	0.000	6.727E-05	NO FIRE
NO IDLE	0.00	0.00	0.192	0.000	6.727E-05	0.192	0.000	6.727E-05	NO FIRE
NO IDLE	0.00	0 00	0.192	0.000	6 727E-05	0.192	0.000	6.727E-05	NO FIRE
NO IDLE	0.00	0.00	0 192	0.000	6 727E-05	0.192	0.000	6 727E-05	NO FIRE
NO IDLE	0.00	0.00	0.192	0.000	6.727E-05	0.192	0.000	6.727E-05	NO FIRE
NO IDLE	0.00	0.00	0.192	0.000	6.727E-05	0.192	0.000	6.727E-05	NO FIRE
NO IDLE	0.00	0.00	0.192	0.000	6.727E-05	0.192	0.000	6.727E-05	NO FIRE
NO IDLE	0.00	0.00	0.192	0.000	6.727E-05	0.192	0.000	6.727E-05	NO FIRE
NO IDLE	0.00	0.00	0.192	0.000	6.727E-05	0.192	0 000	6.727E-05	NO FIRE
NO IDLE	0.00	0.00	0.192	0.000	6.727E-05	0.192	0 000	6 727E-05	NO FIRE
NO IDLE	0.00	0.00	0.192	0.000	6.727E-05	0.192	0.000	6.727E-05	NO FIRE
NO IDLE	0.00	0.00	0.192	0.000	6.727E-05	0 192	0.000	6 727E-05	NO FIRE
NO IDLE	0.00	0.00	0.192	0.000	6.727E-05	0.192	0.000	6 727E-05	NO FIRE
NO IDLE	0.00	0.00	0.192	0 000	6.727E-05	0.192	0.000	6 727E-05	NO FIRE
NO IDLE	0.00	0.00	0.192	0.000	6 727E-05	0.192	0.000	6.727E-05	NO FIRE
NO IDLE	0.00	0.00	0.192	0.000	6.727E-05	0.192	0.000	6.727E-05	NO FIRE
NO IDLE	0.00	0.00	0.192	0.000	6.727E-05	0.192	0.000	6.727E-05	NO FIRE
YES	7,078.58	31.64	0.304	0.000	1 065E-04	0.263	0.000	9.201E-05	NO FIRE
YES	13,177.29	46.08	0.488	0.000	1 709E-04	0.446	0.000	1.564E-04	NO FIRE
NO - 90.96%	24,203.28	43.12	0.730	0.066	2.327E-04	0.618	0.056	1.969E-04	1.3
NO - 0.00%	0.00	46.34	1 017	1.017	2.252E-11	0.875	0.875	1.939E-11	1.7
NO - 0.00%	0.00	45.03	1.161	1.161	2.035E-11	1.115	1.115	1.954E-11	1.3
NO - 0.00%	0.00	66.90	1.085	1.085	1.990E-11	1 053	1 053	1.929E-11	2.3
NO - 0 00%	0 00	11.74	0.476	0.476	2.533E-11	0 378	0.378	2.012E-11	0.6
NO - 0.00%	0.00	19.94	0.596	0 596	2.317E-11	0.508	0.508	1.977E-11	0.7
NO - 0 00%	0.00	56.72	1.213	1.213	2 018E-11	1.175	1.175	1.955E-11	1.6
NO - 0.00%	0.00	24.57	0.884	0.884	2.434E-11	0.720	0 720	1 984E-11	0.7
NO - 0.00%	0.00	27.10	0.570	0.570	2.280E-11	0.497	0.497	1.986E-11	0.9
NO - 0.00%	0.00	9.15	0.400	0.400	2.759E-11	0.314	0.314	2.168E-11	0.6
NO - 0 00%	0.00	-4.52	0.303	0.303	4 906E-11	0.303	0.303	4.906E-11	4.0
NO - 0 00%	0.00	-10 16	0.296	0.296	1 091E-10	0.296	0.296	1.091E-10	4.0
NO - 0.00%	0.00	-10 30	0.289	0.289	1.172E-10	0.289	0.289	1 172E-10	4.0
NO - 0.00%	0.00	-7.67	0.283	0.283	7.551E-11	0.283	0.283	7.551E-11	4.0
NO - 0 00%	0.00	-10.54	0.276	0.276	1.348E-10	0.276	0.276	1 348E-10	4.0
	-22,062.80	-69.00	0.246	0 000	8 621E-05	0.246	0.000	8.621E-05	4.0
	-9,321.18	-51.03	0.226	0.000	7.920E-05	0.226	0.000	7 920E-05	4.0
YES	4,333.78	4.79	0.246	0 000	8.632E-05	0.167	0.000	5.858E-05	NO FIRE
YES	9,379.31	9.03	0.397	0.000	1.393E-04	0.313	0.000	1 097E-04	NO FIRE
YES	12,065.20	9.49	0.408	0.000	1.430E-04	0.325	0.000	1.140E-04	NO FIRE
NO - 18.17%	5,605.68	13.57	0.458	0.375	2.916E-05	0.363	0.297	2.309E-05	0.6
NO - 0 00%	0.00	25.80	0.646	0 646	2.318E-11	0.548	0.548	1.966E-11	0.9
NO - 0 00%	0.00	44 28	1 028	1.028	2.253E-11	0.892	0.892	1.956E-11	1.5
NO - 0 00%	0 00	44 62	1.094	1 094	2.124E-11	1.010	1.010	1.962E-11	1.3
NO - 0.00%	0.00	53.92	0 941	0.941	2.268E-11	0 813	0.813	1.959E-11	1.7
NO - 0.00%	0 00	11.97	0 430	0.430	2.603E-11	0.334	0.334	2.024E-11	0.6
NO - 0.00%	0.00	1.12	0 342	0.342	3.479E-11	0.252	0.252	2 565E-11	1.5
NO - 0.00%	0.00	3.79	0 359	0.359	3.158E-11	0.249	0.249	2.190E-11	0.8
	-9,882.84	-28.95	0 293	0 000	1 028E-04	0 293	0 000	1.028E-04	4.0
	-14,656.19	-55.57	0 267	0.000	9 356E-05	0.267	0.000	9 356E-05	4 0
	-8,797.92	-45.43	0.247	0.000	8 656E-05	0.247	0.000	8 656E-05	4.0
	-4,068 83	-29.96	0.234	0.000	8 211E-05	0.234	0.000	8.211E-05	4 0
YES	4,518.13	4.96	0.262	0.000	9.195E-05	0.180	0.000	6.305E-05	NO FIRE
YES	22,301 40	57.68	0 786	0 000	2.753E-04	0.670	0 000	2.349E-04	NO FIRE
NO - 18.70%	10,586.25	43.39	1.044	0.848	6.840E-05	0.921	0.749	6.036E-05	1.3
NO - 0.00%	0.00	40.65	1.075	1.075	2.167E-11	0.974	0.974	1.963E-11	1.2
NO - 0.00%	0.00	54.04	0.959	0.959	2.252E-11	0.830	0.830	1.951E-11	1 8
NO - 0.00%	0.00	34.33	0.779	0.779	2.434E-11	0.626	0.626	1.956E-11	1.2
NO - 0 00%	0.00	17.90	0.523	0.523	2.385E-11	0.435	0 435	1.984E-11	0.6
NO - 0.00%	0.00	15.22	0.501	0.501	2 442E-11	0.409	0 409	1.992E-11	0.6
NO - 0.00%	0.00	9.76	0.447	0.447	2.627E-11	0.347	0.347	2.041E-11	0.6
NO - 0.00%	0 00	-3.88	0.336	0.336	4.312E-11	0.336	0.336	4 312E-11	4 0
NO - 0 00%	0.00	4 26	0.388	0.388	2.984E-11	0.277	0.277	2.134E-11	0.6
NO - 0.00%	0.00	12.42	0 467	0.467	2.528E-11	0 369	0.369	1.998E-11	0.6
NO - 0.00%	0.00	9.71	0.442	0.442	2.635E-11	0.343	0.343	2.040E-11	0 6
NO - 0 00%	0 00	4 31	0.391	0.391	2.967E-11	0.281	0.281	2.135E-11	0.6
NO - 0.00%	0.00	4.28	0.389	0.389	2.976E-11	0.279	0.279	2.135E-11	0 6
NO - 0.00%	0 00	6.97	0.413	0.413	2.783E-11	0.321	0.321	2.163E-11	0.5

Appendix D - Detailed Description of Unit Processes Involved in an Air Braking/Driving Event

In an attempt to analyze air braking and air driving events in more detail than that provided by an available energy analysis, the processes involved in the operation of the pneumatic hybrid engine were modeled as a sequence of simpler thermodynamic processes. In this section, we categorize the steps involved in air braking/driving events (described in Chapter 4) into several unit processes. Furthermore, the goal of this Appendix is to show the reader the algebraic derivations that were used to generate the formulas in Chapter 4.

The list of symbols on page 8 does not necessarily apply to the contents of this section. All terms appearing on the equations to follow are defined locally. As before, the symbols P, T, V, and m refer to pressure, temperature, volume, and mass, respectively. Moreover, the subscripts i and f stand for initial and final values, where the initial values of the states are always known. Whenever air flows from one tank to another, the letters S and D correspond to source and destination. In that case, three subsystems, *I*, *II*, and *III*, are defined. These are the mass of air that begins and ends at S, the mass transferred from S to D, and the air that stays in D throughout the whole process. The symbol M denotes the total mass of air involved in the mass transfer process, that is, the combined mass of subsystems *I*, *II*, and *III*. Ultimately, the symbols used within each subsection are independent from those used within the others unless it is stated otherwise.

(1) Adiabatic Reversible Compression/Expansion Process

Adiabatic reversible compression and expansion processes of the kind described in this subsection occur in process 1-2 of a braking event and process 4-5 of an air driving event as described in Chapter 4. Figure D-1 shows a schematic of the piston-cylinder device used in this process.

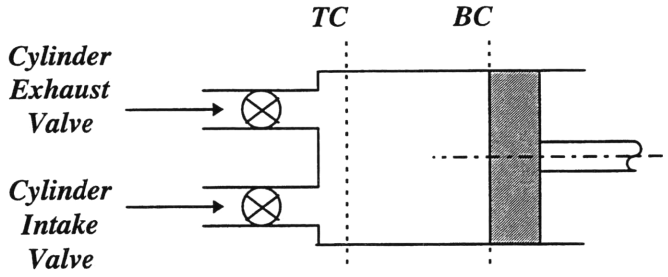

Figure D-1. Engine Cylinder

For initial cylinder pressure P_i, temperature T_i, and volume V_i, if the contents of the cylinder are compressed or expanded to a volume V_f, the final air pressure and temperature are determined via

$$P_f = P_i\left(\frac{V_i}{V_f}\right)^{\gamma}$$
$$T_f = T_i\left(\frac{V_i}{V_f}\right)^{\gamma-1}. \tag{D.1}$$

From the ideal gas law, we know that the mass of air inside the cylinder is given by

$$m = \frac{P_i V_i}{RT_i}. \tag{D.2}$$

Ultimately, the first law of thermodynamics for closed systems yields that the net amount of work done by the air on the piston in this type of process is

$$W_{net} = mc_v\left(T_i - T_f\right) + P_a\left(V_i - V_f\right) = \frac{c_v}{R}\left(P_i V_i - P_f V_f\right) + P_a\left(V_i - V_f\right), \tag{D.3}$$

where the second term on the right accounts for the work done on or by the atmosphere as the piston moves. The available energy of the system increases/decreases (depending upon whether compression or expansion is taking place) by the magnitude of W_{net}, since the process above is reversible.

(2) Adiabatic Instantaneous Blowdown Process

The following process description applies to processes 2-3 and 4-5 in a braking event and to processes 1-2 and 2-3 in an air driving event. Figure D-2 shows a schematic of the system used to calculate the states of the air after an adiabatic instantaneous blowdown process.

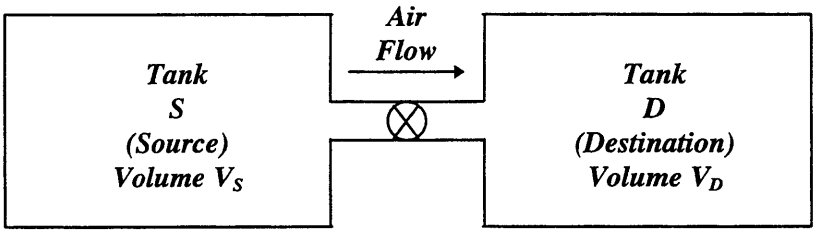

Figure D-2. Schematic of Two Tanks Involved in a Blowdown Process

The system above consists of 3 subsystems, *I*, *II*, and *III*. Subsystems *I* and *III* remain in tanks *S* and *D*, respectively, throughout the whole process. The air in subsystem *II* is transferred from *S* to *D*, and an irreversible mixing process occurs in tank *D*. Mechanical equilibrium is attained between both tanks at the end of the process. Since the system is closed and the

blowdown process is adiabatic, there is no change in its total energy. Thus, from the first law of thermodynamics, we have that

$$c_v\left[m_I\left(T_{S_f}-T_{S_i}\right)+m_{II}\left(T_{D_f}-T_{S_i}\right)+m_{III}\left(T_{D_f}-T_{D_i}\right)\right]=0. \tag{D.4}$$

Applying the ideal gas law and substituting into Eq.(D.4), we get, in terms of the known tank volumes and of initial and final pressures, that

$$\left(P_{S_f}-P_{S_i}\right)V_S+\left(P_{D_f}-P_{D_i}\right)V_D=0\Leftrightarrow P_{S_f}=P_{D_f}=P_f=\frac{P_{S_i}V_S+P_{D_i}V_D}{V_S+V_D}. \tag{D.5}$$

Subsystem I undergoes an adiabatic reversible expansion. Consequently, its final temperature satisfies the relationship

$$P_{S_i}^{1-\gamma}T_{S_i}^{\gamma}=P_f^{1-\gamma}T_{S_f}^{\gamma}\Leftrightarrow T_{S_f}=T_{S_i}\left(\frac{P_f}{P_{S_i}}\right)^{1-\frac{1}{\gamma}}, \tag{D.6}$$

where P_f is given by Eq.(D.5). From the ideal gas law, we have, in terms of known quantities,

$$M=\frac{1}{R}\left(\frac{P_{S_i}V_S}{T_{S_i}}+\frac{P_{D_i}V_D}{T_{D_i}}\right),$$

that

$$m_I=\frac{P_{S_f}V_S}{RT_{S_f}},\ \text{and} \tag{D.7}$$

$$m_{III}=\frac{P_{D_i}V_D}{RT_{D_i}}$$

Therefore,

$$m_{II}=M-m_I-m_{III}. \tag{D.8}$$

Finally, the ideal gas law yields that the final temperature in tank D is

$$T_{D_f}=\frac{P_fV_D}{(m_{II}+m_{III})R}. \tag{D.9}$$

The decrease in available energy of the system resulting from the irreversible blowdown process is determined via

$$\Delta W_{ava_{SD}}=\left(W_{ava_{S_i}}+W_{ava_{D_i}}\right)-\left(W_{ava_{S_f}}+W_{ava_{D_f}}\right), \tag{D.10}$$

where the values for the available energy terms may be calculated using the method described in Section 2.1.

(3) Adiabatic Reversible Compression/Expansion of the Contents of 2 Tanks

The type of process that will be analyzed in this subsection is that in which two tanks at the same known pressure but with contents at different, also known, temperatures are connected

together and compressed or expanded adiabatically and reversibly by a piston. This refers to process 3-3' both in an air braking and an air driving event. After the compression/expansion process, although gas flows from one tank into the other, no mixing occurs inside the destination tank. Figure D-3 illustrates the 2-tank model used to analyze processes of type (3). The picture shows the configuration corresponding to the compression (braking) case.

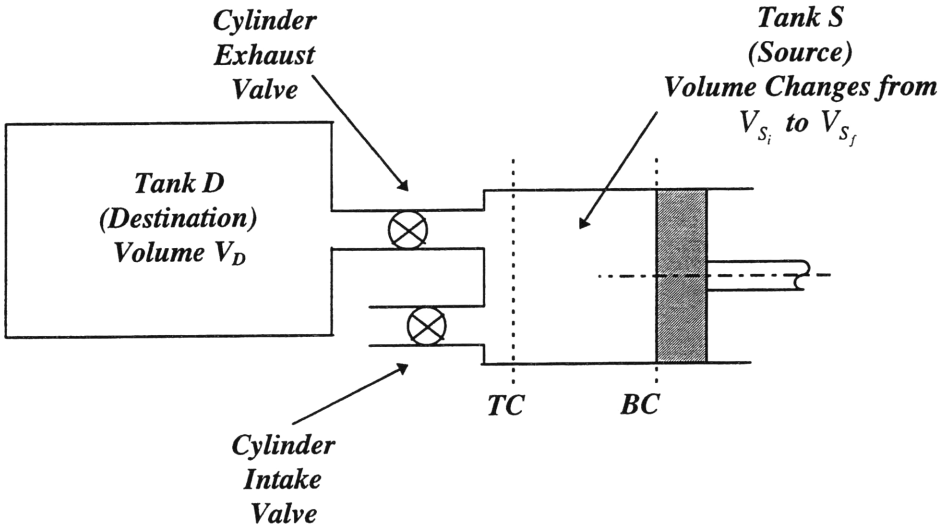

Figure D-3. Physical Model Used to Analyze a Reversible Adiabatic Compression/Expansion of the Contents of Two Tanks

The definition of subsystems *I*, *II*, and *III* from subsection (2) applies. However, for an expansion process, tanks *S* and *D* as shown in Fig. D-3 are interchanged. For an adiabatic reversible compression/expansion process, we have that

$$P_{D_f} = P_{S_f} = P_f = P_i \left(\frac{V_{S_i} + V_D}{V_{S_f} + V_D} \right)^{\gamma} . \tag{D.11}$$

The 3 subsystems undergo the same type of compression/expansion process. Consequently, Eq.(D.6) acquires the following form:

$$T_{I_f} = T_{S_f} = T_{I_i}\left(\frac{P_f}{P_i}\right)^{1-\frac{1}{\gamma}} = T_{S_i}\left(\frac{P_f}{P_i}\right)^{1-\frac{1}{\gamma}},$$

$$T_{II_f} = T_{S_i}\left(\frac{P_f}{P_i}\right)^{1-\frac{1}{\gamma}}, \text{ and} \qquad (D.12)$$

$$T_{III_f} = T_{D_i}\left(\frac{P_f}{P_i}\right)^{1-\frac{1}{\gamma}}$$

The masses m_I, m_{II}, and m_{III} are again defined by Equations (D.7) and (D.8), although they do not necessarily have the same values as those. The net amount of work done by the air inside the two tanks is obtained, via the same procedure described in subsection (1), by

$$W_{net} = \frac{c_v}{R}\left[P_i\left(V_{S_i} + V_D\right) - P_f\left(V_{S_f} + V_D\right)\right] + P_a\left(V_{S_i} - V_{S_f}\right). \qquad (D.13)$$

Like the process described in (1), the available energy of the system in Fig. (D.3) changes according to the quantity in Eq.(D.13), since the compression/expansion process in question is also reversible.

(4) Pure Mixing Process

After the process described in subsection (3) is concluded, a pure mixing process follows. This subsection refers to process 3'-4 in a braking event as well as in an air driving event. Before mixing occurs, two subsystems having generally different mass and temperature but a common pressure are contained together inside a tank, shown in Figure D-4. At the end, the contents of the tank are at a common temperature, and the pressure remains unchanged.

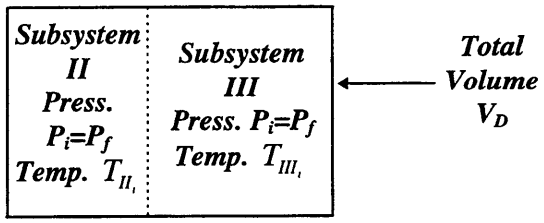

Figure D-4. Tank in which Pure Mixing Process Occurs

The mass of air in subsystem *II* (m_{II}), which represents the mass of air transferred from tank *S* to tank *D* in the process described in subsection (3) is known from (3). Likewise, mass m_{III} is a quantity given from (3). For a system undergoing a pure mixing process, the first law of thermodynamics has that

$$c_v\left[m_{II}\left(T_{D_f}-T_{II_i}\right)+m_{III}\left(T_{D_f}-T_{III_i}\right)\right]=0 \Leftrightarrow T_f=T_{D_f}=\frac{m_{II}T_{II_i}+m_{III}T_{III_i}}{m_{II}+m_{III}}. \quad \text{(D.14)}$$

The amount of available energy lost in this process due to irreversible mixing is calculated from

$$\Delta W_{ava_D}=W_{ava_{D_i}}-W_{ava_{D_f}} \quad \text{(D.15)}$$

using the method described in Section 2.1.

(5) Thermal Equilibration Process

The process of interest in this segment is the exchange of heat between the contents of a tank and its wall. This takes place as process 5-6 in a braking event, in which heat is generally lost to the wall, and as process 6-7 in an air driving event, where, on the other hand, the air that remains inside the tank absorbs heat from the wall. Figure D-5 shows the model used for our calculation.

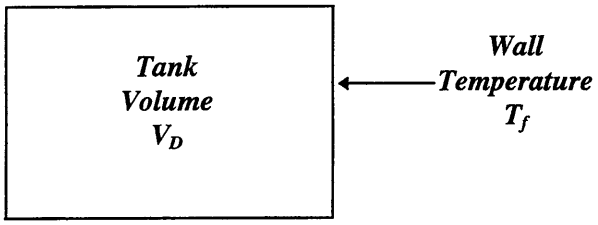

Figure D-5. Model Used for Thermal Equilibration Process

Initially, the tank contains a mass of air m at pressure P_i and temperature T_i. The first law of thermodynamics for a closed system with no mechanical interactions has that, the net amount of heat absorbed by the air from the tank wall is

$$Q=mc_v\left(T_f-T_i\right), \quad \text{(D.16)}$$

where

$$m=\frac{P_iV_D}{RT_i} \quad \text{(D.17)}$$

from the ideal gas law. By the same reasoning, the final air pressure is

$$P_f=\frac{mRT_f}{V_D}. \quad \text{(D.18)}$$

The net loss of available energy in the system consisting of the air tank in Fig. D-5 is given by Eq.(D.15). In the case that T_f is higher than T_i, the air absorbs heat and the result from Eq.(D.15) is negative, since available energy is gained.

(6) Adiabatic Blowdown/Tank Filling Process

In an air driving event, the "exhaust valve" of the cylinder in use opens at the end of the expansion stroke, a point denoted at state 5 in Chapter 4. After this happens, either a blowdown or a tank filling process occurs, denoted as process 5-6, depending upon whether the cylinder pressure at state 5 is above or below atmospheric level, respectively. As discussed in Chapter 4, the former case is preferred, although the no blowdown case is ideal.

Figure D-6 shows a schematic of the model used to predict the final state of the air after undergoing process 5-6 in an air driving event. Throughout the process, the cylinder volume remains at its maximum value, V_c+V_d. For known initial air pressure and temperature, the ideal gas law states that

$$m_i = \frac{P_i\left(V_c + V_d\right)}{RT_i}. \tag{D.19}$$

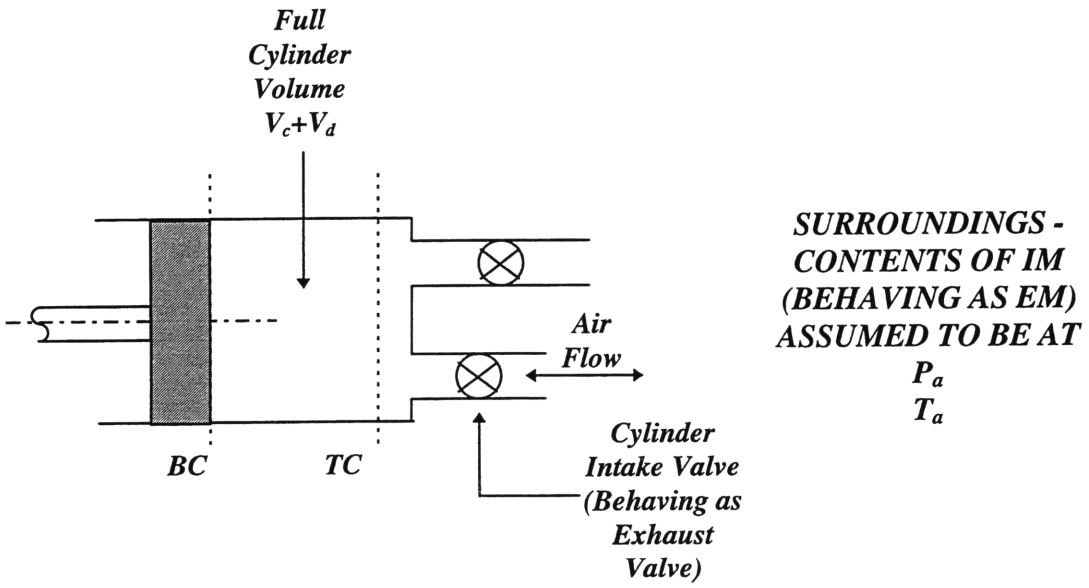

Figure D-6. Physical System Involved in Process 5-6 of an Air Driving Event

For the case in which $P_i > P_a$, air will flow out of the cylinder. The subsystem consisting of the mass of air that remains in the cylinder throughout the process undergoes an adiabatic reversible expansion. Consequently, the final temperature and mass of air in the cylinder are

$$T_f = T_i\left(\frac{P_a}{P_i}\right)^{1-\frac{1}{\gamma}}$$
$$m_f = \frac{P_a\left(V_c + V_d\right)}{RT_f}, \tag{D.20}$$

since $P_f = P_a$.

In the case that $P_i < P_a$, air at atmospheric conditions will flow into the cylinder. The first law of thermodynamics for open adiabatic systems, Eq.(A.1), states for this case, after integrating, that

$$c_v\left(m_f T_f - m_i T_i\right) = c_p T_a\left(m_f - m_i\right) = \frac{c_v}{R}\left(P_a - P_i\right)\left(V_c + V_d\right) = c_p T_a\left[m_f - \frac{P_i\left(V_c + V_d\right)}{RT_i}\right] \Leftrightarrow$$
$$m_f = \frac{V_c + V_d}{R}\left(\frac{P_a - P_i}{\gamma \cdot T_a} + \frac{P_i}{T_i}\right) \tag{D.21}$$

The final temperature of the air remaining in the cylinder may be obtained from the second equation in (D.20) using the result from Eq.(D.21).

After the blowdown/tank filling process is concluded in the cylinder, the piston moves all the way to TC (process 7-8) in order to conclude the cycle. For the contents of the cylinder, this is a constant pressure (atmospheric) and constant temperature (T_f) process. The ideal gas law gives that the mass of air in the cylinder at the end of the process is

$$m_{END} = \frac{P_a V_c}{RT_f}. \tag{D.22}$$

Ultimately, the reduction in the available energy inside the cylinder is given by the difference between the value of this quantity before the blowdown/tank filling process and that after the piston has traveled back to TC. Note that, although the method described in Chapter 2 to calculate available energy is still valid, the mass of air in question changes from beginning to end.